Environmental and Experimental Botany 221 (2024) 105716

Contents lists available at ScienceDirect

Environmental and Experimental Botany

journal homepage: www.elsevier.com/locate/envexpbot

Research paper

Physiological efficiency of grapevine canopies having varying geometries: Seasonal and diurnal whole canopy gas exchange assessment under well-watered and water deficit conditions

F. Del Zozzo, E. Magnanini, S. Poni *

Department of Sustainable Crop Production, Università Cattolica del Sacro Cuore, Via Emilia Parmense 84, Piacenza 29122, Italy

ARTICLE INFO

Keywords:
Vitis vinifera
Photosynthesis
Transpiration
Total light interception
Modeling
Training systems

ABSTRACT

Grapevine training systems should be thoroughly examined to contribute to vineyards more resilient to climate change. This study was conducted on 18 three-year-old fruiting Sangiovese vines grown in pots outdoors with canopies trained to a vertical shoot positioned (VSP) spur-pruned cordon, a single high wire (SHW), and a Pergola (P) training system. Whole-canopy net CO_2 exchange rate (NCER) and transpiration (T) were monitored by an enclosure system on a 24/7 basis from DOY 179–249. All vines were kept well-watered (WW) from DOY 179 to DOY 199, and the water supply was first reduced to 50% (DOY200–204) and then to 35% (DOY 205–214) before final rewatering (DOY 215–217). Vegetative growth, yield components, and grape composition were also assessed. Seasonal gas exchange on a per vine basis reflected vine size given as total leaf area (LA) varying from 2.5 to 3.1 m^2; however, when diurnal trends of NCER/LA and T/LA within the WW and rewatering periods were considered, the good correlations found with the modeled total canopy light interception (TCLI) in SHW and P, were not confirmed in VSP. In all canopy geometries, the best predictor of NCER/LA was the total direct light intensity, whereas T/LA was linearly and closely correlated with air VPD. In terms of NCER/LA during the WW period, SHW had 24% higher rates than VSP and P. Under progressive water stress, SHW again exhibited higher drought resilience, while NCER and T were severely reduced in VSP and P. Severe stress also caused lower light saturation points and quantum yield in VSP and P. Under similar yield levels, P reached the best fruit maturity. In terms of photosynthetic efficiency and adaptive response to increasing water stress, the SHW performed best. Results extrapolated at the field level indicate the P system as the most rewarding.

1. Introduction

Regardless of its size and geometry, a grapevine canopy is a complex population of single leaves having large heterogeneity in age, light exposure, health status, etc., and seasonally and diurnally interacting with weather conditions and cultural practices, among which summer pruning operations, such as shoot thinning and trimming and leaf removal have a primary role (Poni et al., 2023). Thus, choosing the most efficient training system among the more than 40 types described in textbooks (Winkler, 1974) is quite an endeavor for three main reasons: (i) common criteria to define *efficiency* have to be found; (ii) appropriate methodology to integrate the above complexity is needed; and (iii) the role played by climate change needs to be considered when prioritizing certain training systems versus others.

A consensus can be reached if an efficient training system finds the best compromise between light interception and light distribution within the canopy while assuring nonlimiting dry matter partitioning to clusters and renewal wood. A problem arises when comparative evaluation among different training systems is needed. The vast array of existing grapevine training systems can be synthesized into three main types: vertically shoot positioned (VSP), free-growing (sprawl), and semi-horizontal, sloped (pergola type) canopies (Reynolds and Heuvel, 2009).

Methodologies available to assess the efficiency and performances of different grapevine training systems can be summarized according to a top-bottom gradient of increasing complexity as it follows: (i) computation of simple geometrical calculations leading to, for instance, the exposed or external canopy area per meter of row or hectare (Carbonneau, 1983; Smart, 1985); (ii) calculation of the so-called vine balance indices, pioneered by the yield-to-pruning weight ratio, otherwise

* Corresponding author.
E-mail address: stefano.poni@unicatt.it (S. Poni).

https://doi.org/10.1016/j.envexpbot.2024.105716
Received 8 January 2024; Received in revised form 24 February 2024; Accepted 25 February 2024
Available online 27 February 2024

known as the Ravaz index, and having nowadays the leaf area-to-fruit as the most popular (Kliewer and Dokoozlian, 2005); (iii) the advent of 3D reconstruction models (Garcia-Tejera et al., 2023; López-Lozano et al., 2011; Louarn et al., 2008a, 2008b; Mabrouk and Sinoquet, 1998). These models infer canopy structure indices from basic field measurements (e.g., leaf azimuth and inclination, leaf number, average shoot leaf area, and length) and dissect the ability of a training system to capture light efficiently. Model outputs can easily be extended to other variables, such as leaf area, yield, and seasonal dry matter partitioning (Cola et al., 2014; Lakso et al., 2007; Poni et al., 2006); (iv) special devices built to address the issue of light interception from specific organs or portions of the canopy (Poni et al., 2015); and (v) direct assessment of whole-canopy gas exchange using an enclosure system (Lloyd et al., 1995).

The latter inherently solves the issue of canopy complexity in a given training system albeit posing methodological challenges (design, setup, calibration, maintenance, etc.) since these systems are not commercially available (Corelli-Grappadelli and Magnanini, 1993; Peña and Tarara, 2004; Poni et al., 1997). The entire canopy is enclosed in a chamber made of different materials (e.g., polyethylene, mylar, polycarbonate, etc.), which is flushed by a continuous air flow adjusted to control overheating while allowing some gas exchange differential to develop. CO_2 and H_2O measured at the inlets and outlets of the chambers then allow a calculation of the net CO_2 exchange rate (NCER), transpiration (T), and canopy water use efficiency as NCER/T. Indeed, several merits can be attributed to this approach when the efficiency of different training systems is the challenge. As Intrieri et al. (1997) claimed, parallel readings taken of single-leaf and whole-canopy gas exchange rates for different training systems are inherently a comparison method. If readings taken on healthy mature single leaves under nonlimiting light and VPD conditions represent the optimal (read maximum) rate, values derived from the whole canopy assessment, once normalized according to a shared unit (for instance, μmol $m^{-2}s^{-1}$ for the photosynthetic rate), will be lower, depending on the incidence of any factor that limits leaf function (too young, too old, pale green or yellow, unhealthy, etc.). Presumably, the larger this gap, the less efficient the training system.

Specific work employing a whole-canopy approach has significantly contributed to clarifying several responses related to different canopy sizes, density, orientation, and manipulation within a given trellis or between trellises. To name a few, by mounting chambers on VSP-trained field-grown grapevines with NS-oriented rows, Petrie et al. (2009) found that the expected bimodal diurnal patterns found in clear days were not evident on cloudy days when, interestingly, the vines appeared to be more efficient, photosynthesizing at a higher rate per calculated unit of light intercepted. Also, a whole-canopy approach has been profitably used to assess, mostly under VSP training, the complex changes that summer pruning is causing seasonally and that a single-leaf approach would be unlikely to represent effectively (Poni et al., 2023). Thus, responses have been clarified for traditional leaf removal and shoot topping (Petrie et al., 2003), early leaf removal (Poni et al., 2008), apical to the cluster leaf removal (Poni et al., 2013), shoot thinning (Bernizzoni et al., 2011), row orientation (Intrieri et al., 2015), and conventional versus minimal pruning (Poni et al., 2000).

Fewer examples are available where whole vine chambers have been mounted to include different training systems within the same experiment. The comparison is still mostly limited to VSP vs. SHW (Intrieri et al., 1997; Louarn et al., 2008a; Prieto et al., 2020). A common trait to these studies, albeit conducted with different cultivars and growing conditions, is that if the SHW is figured out as a mostly erect canopy eventually trimmed to prevent downward growing, the same benefits from a 25%–30% higher sunlit leaf area that would also warrant better photosynthetic performances. Recent work (Petrie et al., 2023) has compared vine gas exchange for Sauvignon blanc vines trained to VSP and Scott-Henry (SH), indicating that the greater the leaf area of SH-trained vines, the higher the vine photosynthesis in the morning and afternoon, while little effect was found during the central hours of the day.

Choosing a given training system over others might also represent a valuable approach to adapting to climate change. Renowned training systems, such as goblet and VSP, the latter characterized by its short and long (Guyot) pruning management, maintain a leading role when premium still wines are the main target. Yet, mostly due to the impact of climate change, they are showing increasing weaknesses, which often require modifications in canopy management (Poni et al., 2023) or retrofitting to other trellises. The typically featured low cordons increase the risk of frost damage, whereas the low yield levels (especially in goblets) contribute to earlier ripening under the risk of untypical traits while showing little or no potential to exploit a longer growing season. In VSP canopies, regardless of the pruning type, a given row side will be exposed in summer, sooner or later, to the issues of overheating and/or sunburn, regardless of row orientation. The mentioned potential weaknesses suggest that modern training systems where features of higher cordons, slightly higher productivity, and a partial cluster leaf cover are deemed to be desirable should be revisited.

Hence, the current study aims to (i) determine if and how a change in grapevine canopy geometry affects seasonal and diurnal whole vine gas exchange under well-watered and water stress conditions; (ii) establish functional relationships between environmental variables and gas exchange; and (iii) update guidelines in training system recommendations within a global warming scenario.

2. Materials and methods

2.1. Plant material and experimental layout

The experiment was conducted in 2023 at the Department of Sustainable Crop Production (DIPROVES) of the Università Cattolica del Sacro Cuore in Piacenza, (45°02' N, 9°43' E, 54 m asl), on 18 three-year-old cv. Sangiovese, clone VCR102 grafted on SO4, grapevines (*Vitis vinifera* L.) grown outdoors in 45 L pots. The pots were square-shaped to minimize root curling and painted white to prevent excessive temperature rise in summer. The soil mix texture was 83% sand, 10% loam, and 7% clay with 1.83% organic matter and hydrological constants calculated after Saxton and Rawls (2016) were 5.4% (wilting point) and 11.2% (field capacity), resulting in 0.083 cm/cm of available water. Pot available water was finally estimated at 3.8 L.

The vines were randomly assigned to the three following treatments (6 vines each), corresponding to three different canopy geometries (Figure S1): the Single High Wire (SHW) and the Vertically Shoot Positioned (VSP) training systems, sharing a unilateral permanent cordon per vine with five to six two-node spurs to give about 10–12 count nodes per vine. In SHW, a cordon was trained at 1.7 m above ground, and no upper foliage wires were used (Fig. S1 A, G). The VSP cordon height was 0.9 m above ground and surmounted by three foliage wires extending about 1.1 m from the main wire (Fig. S1B, H). The Pergola (P) trained vines featured one two-node renewal spur and two externals, perpendicularly oriented to the row axis, five- to six-node canes tied on a metal wired frame at 20° of inclination concerning the horizontal plain. The vine head was set at about 1.4 m, extending at about 1.6 m at the end of the supporting frame (Fig. S1 C, I).

As per canopy management, in SHW, shoots were trimmed at the seventh to eighth node when they were still mostly vertical to promote and maintain the semi-erect growth habit typical of a spreading canopy. In VSP, vines were trimmed once the shoots outgrew the top foliage wire setting for a canopy about 1.2 m tall. In the cane-pruned Pergola vines, the main developing shoots were trimmed once they exceeded the 1.1–1.2 m distance from the row axis. No trimming was applied to shoots vertically arising from the fruiting canes.

SHW and VSP vines have an NE-SW orientation (215° azimuth), whereas the Pergola canopies were NW-SE-oriented (125° azimuth). Due to the limited space available on the outdoor platform, no adjacent rows for each canopy type at standard spacing (e.g., 2.5 m) could be set;

however, care was taken to exclude that mutual shading from any adjacent canopy could interfere with the light interception potential of the test vines.

Throughout the whole trial encompassing the DOY 178–221 (27 June–9 August) period, vines pertaining to the three canopy geometries were subjected to the following irrigation regimes: well-watered (WW) vines received 4.5 L/day for all trials, which is about 20% above than the estimated pot water capacity (3.8 L). More specifically, one emitter per pot (Shrubbler® 360° Antelco, Adelaide, Australia) was used for automated water supply at 8:00 a.m., 1:00 p.m., and 6:00 p.m. Each irrigation event lasted three minutes, and at a rate of 500 mL min^{-1} per emitter, it supplied 1,5 L/vine. Water Stress (WS) vines had their daily water supply gradually reduced from 100% (DOY 179–199) to 50% (DOY 200–204 to correspond to 2.25 L/vine), to 35% (205–214, to correspond to 1.87 L/vine) then followed by full rewatering (215–217). Within each canopy type, WS treatment was randomly assigned to three of the six vines available. Reduction of water supply was achieved by automated shortening of the duration of irrigation events.

2.2. Vine water status, whole canopy gas exchange, and modeled total canopy light interception

Leaf water status was checked at selected dates, representing the different levels of water stress and rewatering (DOYs 198, 201, 208, 210, and 216), utilizing a Schölander pressure bomb (Soilmosture Equipment Corp., Santa Barbara, CA, USA). Thanks to the zip-lock access on one side of each chamber, leaves could be sampled randomly from the same vines where gas exchange monitoring was undergoing. On each day of measurement, 1 h before dawn (4:30 a.m.) and around solar noon (1:00–2:00 p.m.), three mature, mid-shoot positioned leaves per vine were selected to determine pre-dawn (Ψ_{PD}) and midday (Ψ_{MD}) leaf water potential. Upon midday readings, leaves were first wrapped with a plastic bag, detached at the petiole with a razor blade, and then quickly inserted into the chamber for measurements.

Whole-canopy net CO_2 exchange rate (NCER) and transpiration (T) were measured using the modified enclosure chamber method described in Poni et al. (2014). In brief, the system features centrifugal blowers (Vorticent C25/2 M Vortice, Milan, Italy) collecting air from a common 1000 L plastic tank and delivering a maximum airflow of 950 $m^3 \cdot h^{-1}$ to fill the chambers; 18 transparent polyethylene chambers were crafted around the canopy allowing 88% light transmission and 6% diffuse light enrichment and no alteration of the light spectrum (Figure S1); a CIRAS 3-DC CO_2/H_2O differential gas analyzer (PP-Systems, Amesbury, MA, USA); and a CR1000 data logger wired to an AM16/32B Multiplexer (Campbell Scientific, Shepshed, England). Every complete reading cycle lasted 21 minutes since the 18 solenoid valves commuted air flow from one chamber to another every 80 seconds. To keep the airflow fed to the chambers the most constant, 18 circular regulators with adjustable constant flow RAD2 100 BP 15–50 m^3/h (France Air Italia, Monza Brianza, Italy) were inserted into the air tube before the air inlet of each chamber. The airflow was set at 13.8 L/s for all chambers and maintained unaltered for the whole measurement period. Temperature was measured by shielded 1- or 0.2 mm diameter perfluoro alkoxy Teflon insulated type-T thermocouples (Omega Engineering Stamford, CT, USA) at the air inlet and each chamber's outlet. In addition, a BF2 sunshine sensor (Delta-T Devices, Cambridge, England) was placed on top of a vertical support, clear from any shadow, and close to the chambers for measuring total direct and diffuse radiation.

Each vine was enclosed in a chamber on DOY 179 (28 June) and operated 24/7 until DOY 218 (6 August, day of dismantling) with minimal interruptions due to either damage caused by heavy thunderstorms with strong winds (i.e., DOY 180) or minor maintenance interventions. Thus, whole-canopy measurements lasted for 37 days. Whole-canopy NCER (μmol s^{-1}) and T (g $hours^{-1}$) from airflow and CO_2 and H_2O differentials were calculated according to Long and Hallgren (1985). Daily gas exchange means were calculated by averaging data taken from dawn to dusk.

At harvest, all main and lateral nodes were counted per vine, and three shoots per vine were sampled and brought to the laboratory. The leaf area on each node of the main and lateral shoots was measured with a leaf area meter (LI-3000 A, LI-COR Biosciences, Lincoln, NE, USA). Afterward, the average leaf area was calculated for main and lateral shoots, respectively. The total leaf area per vine was calculated by multiplying the node number by the average leaf blade area. Since the gas exchange readings started at a time (DOY 179, 28 June) when canopies had almost reached their final size, all gas exchange data was also given on a per leaf area (LA) basis for normalization against absolute leaf area development.

2.3. Modeled total canopy light interception (TCLI)

Modeled direct radiation intercepted by vertical and horizontal planes of each canopy type and diffuse light was calculated in this study by feeding equations and functions, as reflected in Table S1, into a custom-built Mathcad computer program (PTC, Boston, US). The geometrical approach followed to calculate components of solar radiation interception by the vine canopy and distinguished as direct horizontal, direct vertical and diffuse is shown in Figure S2. The example provided in Table S1 refers to the Piacenza location and the DOY 178. Modeling of intercepted light was provided for the whole pre-stress (DOY179–199) and rewatering (DOY 215–2017) periods and outputs were correlated with actual averaged NCER/vine and T/vine values. Some other elementary vineyard features, such as geographical coordinates, main slope, exposure, row orientation, maximum canopy thickness, maximum canopy height, and distance between rows were also needed. Canavera et al. (2023) validated the modeling approach compared to the measured canopy light interception taken in a VSP vineyard located in Piacenza, with rows spaced 2.5 m apart, with a ceptometer over three measuring days (30 June, 8 July, and 18 September) and within each date, over six readings taken at two-hour intervals from 8:00 a.m. to 6:00 p.m. The linear equation forced through the origin was: $y = 0.9938x$, $R^2 = 0.97$.

2.4. Yield components and grape composition

Harvest was performed DOY 244 (01 September) at a total soluble solids concentration (TSS) around 20 Brix. Vine yield was measured with a portable field scale, and the total number of clusters per vine was counted. Six representative clusters per vine were sampled, stored in a cooling bag, and returned to the laboratory for cluster morphology and composition analysis. Clusters were weighted, and rachis length was measured. Cluster compactness was expressed as the ratio of cluster mass to rachis length ($g \cdot cm^{-1}$). The number of berries per cluster was counted to calculate berry mass. Afterward, 60 berries were randomly collected for each vine sample and frozen at −20°C for total anthocyanins and polyphenols analysis. The remaining samples were crushed to obtain a homogeneous must. TSS was assessed with a digital refractometer SMART-1 (Atago, Bellevue, WA, USA), pH was measured with a pH meter (pH 60 VioLab Giorgio Bormac, Carpi, MO, Italy), and titratable acidity (TA), expressed as $g \cdot L^{-1}$ of tartaric acid equivalents, was determined titrating 10 mL of juice solution, with 0.1 N NaOH to a pH 8.2 endpoint, using an AT 1000 Series Potentiometric Titrator (Hach Company, Loveland, CO, USA).

Malic and tartaric acid concentrations were quantified via HPLC (Agilent Technologies, Santa Clara, CA, USA) into auto-sampler vials through a Synergy 4 u Hydro-RP80A column (Phenomenex Inc., Torrance, CA, USA), 250 × 4.6 mm, after juice dilution and 0.22 μm polypropylene syringe filtration. The buffer solution utilized for separation was a 0.2 M KH_2PO_4 adjusted to 2.4 pH with orthophosphoric acid. The column temperature was set at 30°C ± 0.1°C, and a 15 μL sample was injected. The run was performed at 200–700 nm with a diode array detector (DAD) at 210 nm UV. The calibration curve for organic acids

analysis was obtained with external authentic standards via peak areas quantification and the identification of retention time.

Total anthocyanin and polyphenols were determined after Iland (2004). The 60 berries previously frozen were homogenized at 10000 rpm with the Ultra-Turrax T25, (Laboratory Suppliy Network, Atkinson, NH) homogenizer for 1 min. Afterward, 2 g of the homogenate was added with 10 mL of ethanol-water solution (50%, pH 5.0), put into a centrifuge tube, and kept agitating for 1 h before centrifugation at 3500 rpm for 5 min. From the supernatant of the extraction solution, 0.5 mL was collected and added with 10 mL of 1 M HCl, the resultant solution was mixed and after a 3 h rest, absorbance was then measured at 520 and 280 nm on a Jasco V-530 UV spectrophotometer (Jasco Analytical Instruments, Easton, MD, USA). The concentration of the total anthocyanin and polyphenols was expressed as mg per g of berry fresh mass.

2.5. Statistical analysis

Leaf water status, vegetative growth, yield, and grape composition data were subjected to a one-way analysis of variance (ANOVA) using IBM SPSS Statistics 27 (SPSS Inc., Chicago, USA). In the case of the significance of the Fisher test, mean separation was performed through the Duncan Multiple Range Test (DMRT) at $p < 0.05$. Variation around means was given as the standard error (SE).

The regression wizard of the XLSTAT statistical package (Addinsoft, New York, NY, United States) was used for linear and nonlinear regression analyses. Repeated measures of the same parameters (NCER and T on a per vine or leaf area bases) taken at different dates on the same individuals along the study seasons and days were analyzed with the Repeated Measures ANOVA routine embedded in the XLSTAT software package (Addinsoft, New York, N.Y., U.S.A.). Separate analyses were performed for the well-watered measuring period (DOY 179–199) and for the water deficit and rewatering periods (DOY 200–217). Furthermore, the Duncan's Multiple Range Test (DMRT) was used for multiple comparisons within dates at $p < 0.05$. Linear regression slope testing was performed, at $p < 0.05$, by using the T.DIST.2 T function of the Excel package which then returns the two-tailed Student's t-distribution.

3. Results

3.1. Final canopy volumes and modeled diurnal light interception

Canopy volumes were measured at the end of the trial (DOY 218) by annotating canopy length (l), width (w), and height (h). Data shown in Fig. 1 confirm that the SHW had a typical upright, fairly short canopy (volume of 0.280 m^3); VSP had a traditionally narrow and tall vertically shoot-positioned pattern (volume of 0.384 m^3), whereas the Pergola canopy developed within a parallelepiped shape for a total vine canopy volume of 0.374 m^3.

Fig. 2 illustrates the modeled diurnal radiation trends (vertical, horizontal, diffuse component, and resulting total) for the same periods (DOY 179-199, upper panels and DOY 215-217 lower panels) and the three canopy geometries. Magnitude and daily trends of light interception components changes only slightly between the two periods, whereas significant variation occurred between the training systems. The SHW trellis showed an overall bell-shaped pattern in total radiation which, however, is skewed toward the late morning hours (Fig. 2A, D). Horizontally intercepted radiation overtakes vertical radiation from about 9:00 a.m. to 5:00 p.m. For data pooled over the two periods, SHW horizontal radiation accounted for about 50% of the total radiation.

In the VSP canopies, an expected bimodal trend in total radiation was drawn with minimum amounts of light hitting the vertical canopy profile at solar noon, which, at the Piacenza location, occurs at about 1.25 p.m. (Fig. 2B, E). Total radiation trends were again slightly skewed toward the morning hours due to the asymmetry of row orientation

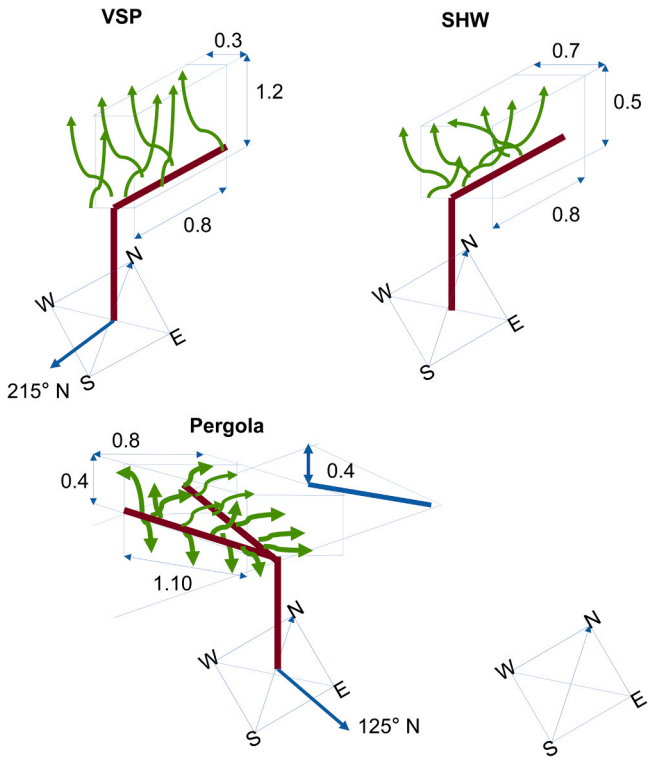

Fig. 1. Schematic diagrams, dimensions (height, width, and length) and orientation of canopy volumes estimated at the end of the experiment for single high wire (SHW), vertically shoot positioned (VSP) and pergola (P) canopies.

versus true North. In VSP, radiation hitting the top section of the canopy exceeded that falling on the vertical plane for a fairly short time window around 2:00 p.m. Horizontally intercepted radiation represented 25% of the total TCLI for the data averaged over the two dates.

The Pergola-trained canopies characterize a pronounced skewness toward the post-midday hours with maximum TCLI reached around solar noon hours (Fig. 2 C, F). In particular, modeled radiation interception suddenly increased right after 10:00 a.m., mostly due to a resumption of vertically intercepted radiation, which had its lowest at 10:00 a.m. In the Pergola canopy system, horizontally intercepted radiation accounted for 50% of total intercepted radiation.

3.2. Seasonal and diurnal whole canopy gas exchange under well-watered condition

Fig. 3A reports the mean daily values of direct and diffuse radiation and air VPD recorded at the experimental site for the whole measuring period (DOY 179–199) during which vines were kept well-watered and, over the same period, as mean diurnal values for the same variables (Fig. 3B). Seasonally, cloudy and relatively cool days were essentially limited to DOY 180, while the remainder of the season showed mean daily total PAR higher than 700 μmol $m^{-2}s^{-1}$ with air VPD reaching out to 3.5 kPa in some very warm days. When evaluated on an averaged diurnal basis, direct PAR had the expected bell-shaped pattern with some minor and temporary lowering, while the still bell-shaped curve for VPD was skewed toward the afternoon hours with a peak reached from 2:00 p.m. to 4:00 p.m. (Fig. 3B).

Seasonal net CO_2 exchange rate (NCER) per vine data (Fig. 3C) processed with repeated measure ANOVA exhibited no significant between-subject (canopy geometry levels) effects ($P = 0.792$), and the same outcome was observed for the diurnal trends averaged over 21 days of pre-stress measurements (Fig. 3D, $P = 0.777$), which, interestingly, had a very similar pattern regardless of the quite different canopy geometries and expected differences in diurnal light interception.

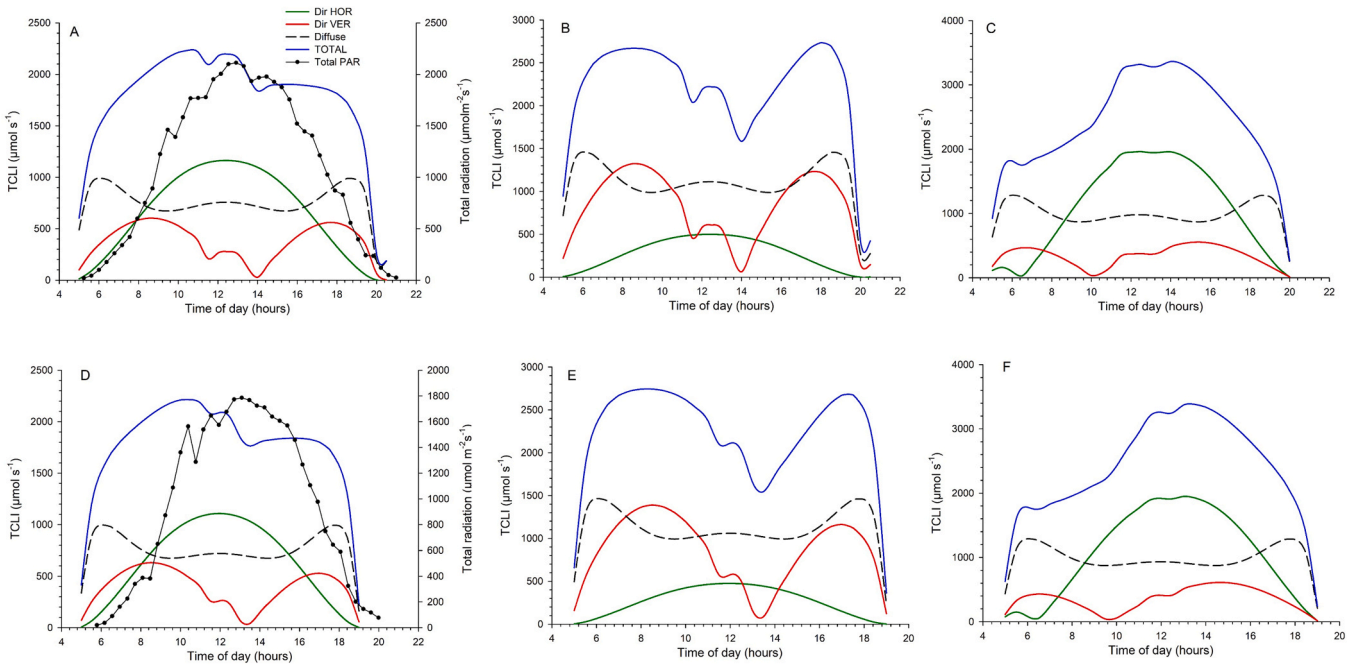

Fig. 2. Simulation of diurnal trends of total direct light on a horizontal (green) and vertical (red), total diffuse (dotted black) and resulting total intercepted light (blue) calculated for the whole pre-stress period (DOY 179-199, upper panels) and the rewatering period (DOY 215-217, lower panels) by Mathcad PLUS 6·0 sofware (Mathsof Inc., Cambridge, MA, USA). For reference, measured total PAR (direct plus diffuse) is shown in panels A and D. At the Piacenza location, average solar noon for the experiment time length occurs at 1.25 p.m., whereas 35 minutes need to be added to get the local time used in the x axis. Panels A, D are SHW, B,E are VSP and C,F are P.

Likewise, no significant dates x treatment interactions were observed. Vice versa, the same interaction was significant for either seasonal (Fig. 3E) and diurnal (Fig. 3F) T/vine at specific measuring dates (indicated with an asterisk in the pertinent figures) with VSP having a consistently higher T/vine than SHW with P allocated at intermediate positions. Daily water use (L/vine) over the whole well-watered period (DOY 179–199) was calculated from the daily hourly rates, as specified in Fig. 4E, multiplied by the average day length, which resulted in 15 h 23'. The resulting mean T per vine was 2.54 L, 3.08 L, and 2.90 L for SHW, VSP, and P, respectively. The above NCER and T patterns determined a tendentially higher seasonal and diurnal canopy WUE in SHW, which reached significance at several dates (Fig. 3G, H).

Gas exchange data were also given, seasonally and diurnally, on a per leaf area basis (Fig. 4A–D) to extract variability due to the absolute amount of foliage and variation in any other intervening factor (light exposure, age, health status, etc.). This could be done as the estimated final leaf area per vine (Table 1) can be considered representative throughout the whole measurement interval as vines had mostly completed their growth by the time the whole canopy gas exchange readings started (i.e. DOY 179, 28 June) due to expected pot root constriction and overall low vigor. Thus, total leaf area (LA) per vine was estimated at 2.26 m^2, 3.16 m^2, and 2.90 m^2 for SHW, VSP, and P, respectively (Table 1).

Fig. 4A shows seasonal NCER/LA trends for each canopy type with consistently higher rates in SHW than the other types, reaching significance from DOY 187–193. NCER/LA averaged over the whole measuring period resulted in 3.74 µmol $m^{-2}s^{-1}$ in SHW, 2.87 µmol $m^{-2}s^{-1}$ in VSP, and 2.99 µmol $m^{-2}s^{-1}$ in P. Thus, SHW had NCER/LA 24% and 20% higher than those measured on VSP and P, respectively. Relative differences among canopy geometries were less pronounced for the T/LA seasonal patterns (dates x treatment interaction was ns) (Fig. 4C).

Diurnal NCER/LA trends averaged over the well-watered measurement period confirmed SHW with the highest rates throughout the day ($p < 0.001$ for time x treatment interaction) although significance was reached only for eight dates (Fig. 4B). All canopy types reached their maximum rates (4–6 µmol $m^{-2}s^{-1}$) around 10:00 a.m. and maintained them fairly constant until about 4:00 p.m. The T/LA was bell-shaped in all training systems, and its peak reached around 2:00 p.m. at 105–135 g m^{-2} $hour^{-1}$ (Fig. 4D). No significant dates x treatment interaction was found.

3.3. Seasonal and diurnal whole canopy gas exchange under stressed conditions and rewatering

The period encompassing progressive water stress and rewatering phases (DOY 200–217) overall showed a majority of clear days with air VPD often comprised between 2 and 2.5 kPa (Fig. 5A–C).

Pre-dawn and midday leaf water potentials measured at different dates throughout the experiment (Table 2) confirmed that reducing the daily water supply to 50% of pre-stress (2.25 L/pot) caused a quite mild level of stress across the canopy forms (DOY 201 data), which remained mild until day 5 of irrigation reduction to 35% of control (DOY 208) and strongly aggravated on DOY 210 when the lowest Ψ_{PD} and Ψ_{MD} were reached in VSP and Pergola. All canopy geometries readily resumed nonlimiting water status upon rewatering.

Seasonal response of NCER/vine to gradual stress and rewatering showed in all canopy systems significant between-treatment and dates x treatment interaction effects, albeit with a significantly different magnitude. In SHW (Fig. 5D), the average NCER/vine calculated over the water stress period (DOY 200, imposition of the 50% water supply until 214, last day at 35% water supply) was 7.72 µmol s^{-1} in WS vs 8.88 in ww (13% less). The same analysis conducted in VSP (Fig. 5E) led to 5.79 µmol s^{-1} in WS and 11.36 µmol s^{-1} in WW (49.1% less), whereas for the Pergola system mean NCER/vine was 6,79 in WS vs 8.93 in WW (24.0% less).

T/vine response over the DOY 200–217 period was somewhat similar (Fig. 5G–I). Throughout the water stress period, fractional reduction in T/vine was 19.5%, 42.3%, and 28.1% in SHW, VSP, and P, respectively, versus the WW treatments. Calculated seasonal canopy WUE (Fig. 5J–L)

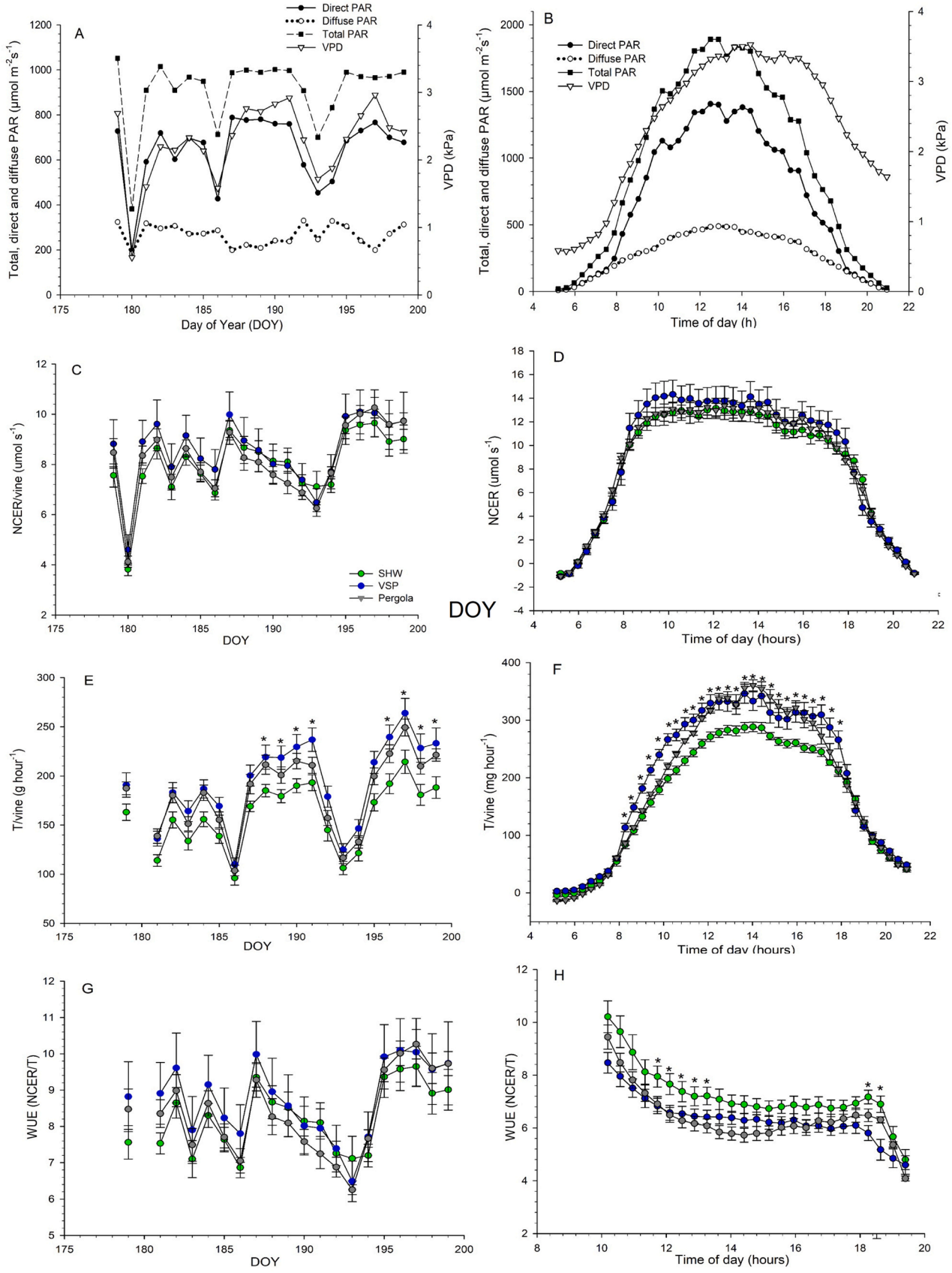

(caption on next page)

Fig. 3. Seasonal (A) and diurnal (B) weather trends as total, direct and diffuse photosynthetic active radiation (PAR) and air vapour pressure deficit (VPD) recorded at the experimental site during the well-watered trial period (DOY 179-199). Seasonal data are averaged from dawn to dusk, whereas diurnal data are daytime averages over 21 days of readings. Panels C, E and G show seasonal NCER/vine, T/vine and WUE (NCER/T), respectively, of the three canopy geometries defined as SHW (green), VSP (blue) and P (dark grey). Data shown in panels C-H were subjected to repeated measure ANOVA and mean separation within date or timing was performed by DMRT (P = 0.05) only when the time x treatment interaction was significant (P = 0.01). Asterisks indicate which dates or timing of the day resulted in significant differences among canopy geometries. Vertical bars represent standard errors (SE) around the means (n = 6). Panels E, F and H registered significant time x treatment interactions according to the following statistics: panel E – time x treatment interaction: F = 3.89, P = 0.001; panel F - time x treatment interaction: F = 8.99, P = 0.01; panel H - time x treatment interaction: F = 3.90, P = 0.01. Data in panels C, D, G were NS.

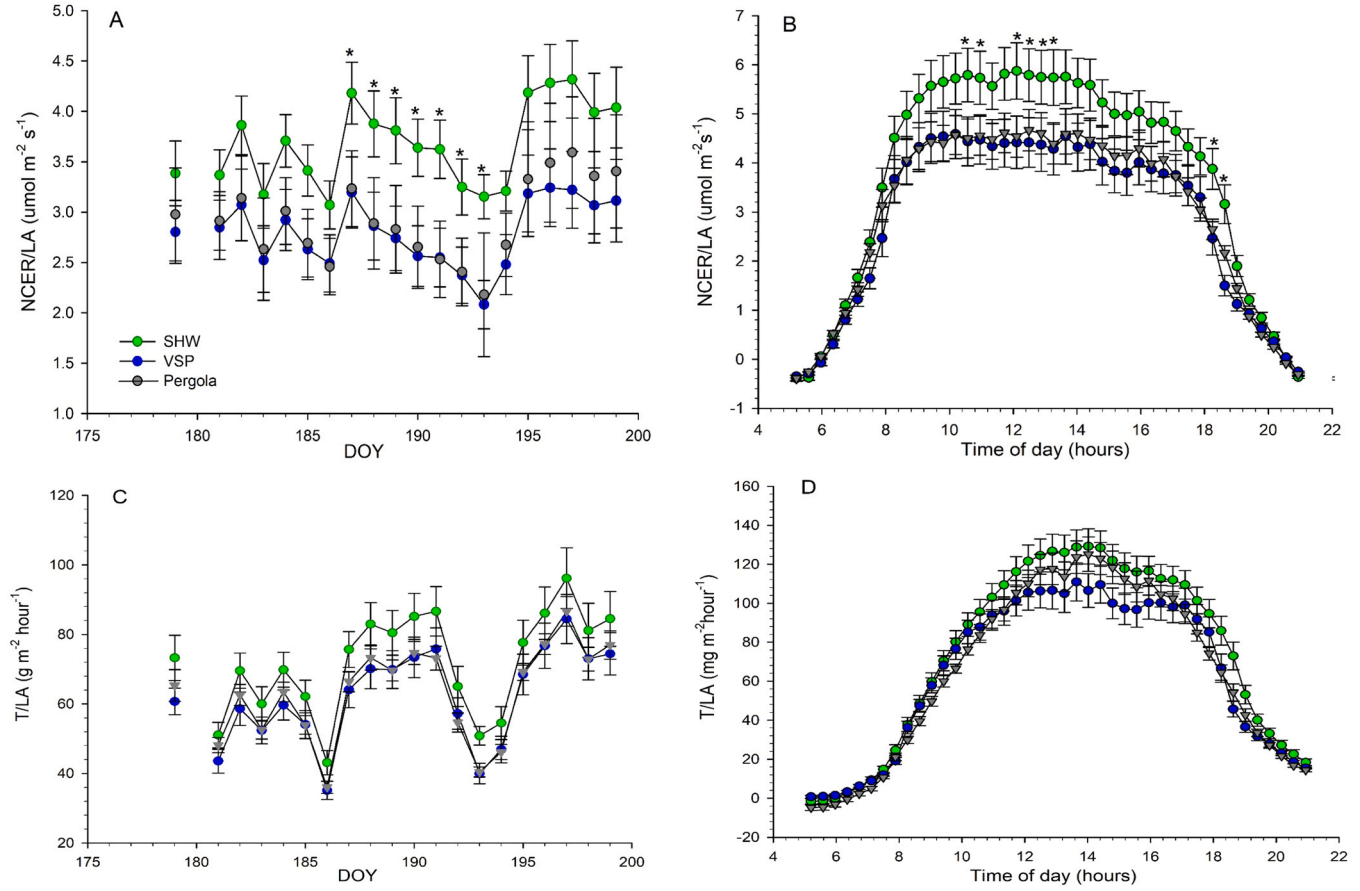

Fig. 4. Seasonal and diurnal patterns of NCER/LA (A,B) and T/LA (C,D) of the three canopy geometries defined as SHW (green), VSP (blue) and P (dark grey). Diurnal patterns (B,D) are averages over the whole pre-stress period (DOY179–199). Data in each panel were subjected to repeated measure ANOVA analysis and mean separation within date or timing was performed by DMRT (P = 0.05) only when the time x treatment interaction was significant (P = 0.01). Asterisks indicate which dates or timings resulted in significant differences among canopy geometries. Vertical bars represent standard errors (SE) around the means (n = 6). Panels A and B registered a significant time x treatment interaction: F = 2.32, P = 0.01 (A); F = 1.93, P = 0.01 (B). Data shown in panels C and D were ns.

Table 1
Data of soil and leaf water status given as pre-dawn leaf water potential (Ψ_{PD}) and midday leaf water potential (Ψ_{MD}), recorded at different dates throughout the pre-stress (DOY 198), moderate stress (DOY 201), severe stress (DOY 208 and 210) and rewatering (DOY 216) periods on potted cv. Sangiovese vines trained as Single-High-Wire (SHW), Vertically Shoot Positioned (VSP) and Pergola (P) training systems.

	Ψ_{PD} (-Mpa) DOY					Ψ_{MD} (-Mpa) DOY				
Treatments	**198**	**201**	**208**	**210**	**216**	**198**	**201**	**208**	**210**	**216**
SHW-WW	0.12c	0.30	0.22b	0.15b	0.15b	0.75	0.77	0.73bc	0.57 d	0.75
SHW-WS	0.13bc	0.30	0.48a	0.45b	0.15b	0.85	0.82	0.75ab	1.46b	0.85
VSP-WW	0.15abc	0.25	0.19b	0.19b	0.15b	0.82	0.75	0.80ab	0.76c	0.82
VSP-WS	0.20a	0.27	0.52a	0.65c	0.15b	0.90	0.80	0.90 a	1.68 a	0.90
Pergola-WW	0.18ab	0.30	0.18b	0.2b	0.14b	0.80	0.80	0.59c	0.69c	0.80
Pergola-WS	0.14b	0.39	0.5 a	0.66c	0.20 a	0.85	0.80	0.88ab	1.76 a	0.85
Dates	F = 350.6; p < 0.001					F = 135.3; p 0.001				
Treatment	F = 832.9; p < 0.001					F = 133.0; P< 0.001				
Treatment x dates	F = 150.3; p < 0.001					F = 45.14; P < 0.001				

Data were subjected to repeated measure ANOVA analysis. In presence of significant (P = 0.001) treatment and treatment x dates effects, mean separation within columns was performed by DMRT test, P = 0.01.

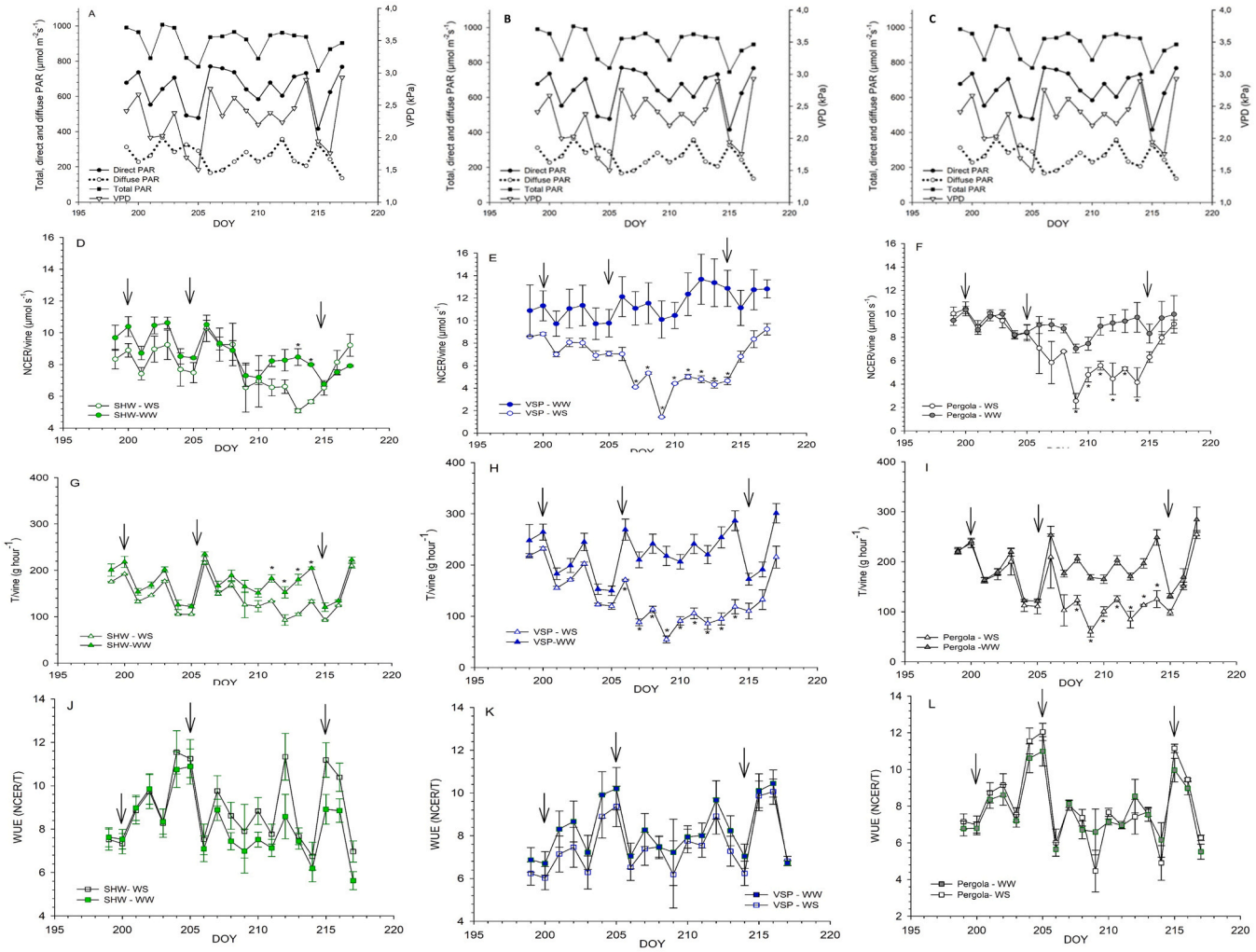

Fig. 5. Seasonal (A and then replicated in B and C) weather trends as total, direct and diffuse PAR and air VPD recorded at the experimental site during the water deficit and rewatering periods (DOY 200–217). Seasonal data are averaged from dawn to dusk. Panels D, J and J show seasonal NCER/vine, T/vine and WUE (NCER/T), for SHW (green); panels E, H, and K refer to VSP (blue) and F, I and L refer to Pergola (dark grey). Data shown in panels D-L were subjected to repeated measure ANOVA analysis and mean separation within date or timing was performed by Fisher test (P = 0.05) only when the time x treatment interaction was significant (P = 0.01). Asterisks indicate which dates resulted in significant differences between water stressed (WS) and well-watered (WW) treatments within each canopy geometry. Vertical bars represent standard errors (SE) around the means (n = 3). Panels D-I registered significant time x treatment interactions according to the following statistics: panel D - time x treatment interaction: F = 14.3, P = 0.001; panel E – time x treatment interaction: F = 19.9, P = 0.01; panel F - time x treatment interaction: F = 8.05, P = 0.01; panel G - time x treatment interaction: F = 3.89, P = 0.01; panel H - time x treatment interaction: F = 73.75, P = 0.001; panel I - time x treatment interaction: F = 39.2, P = 0.01; Data in panels J, K and L were ns. From left to right, arrows indicate beginning of first and second water stress periods and final rewatering.

Table 2
Vegetative growth and yield components determined at harvest on potted cv. Sangiovese vines trained of Single High Wire (SHW), Vertical Shoot Positioned (VSP) and Pergola canopies under Well-Watered (WW) and Water Stress (WS) irrigation regimes.

Treatments (T)	Canes /vine (n)	Main nodes/ vine (n)	Lateral nodes/vine (n)	Total nodes/ vine (n)	Main LA/ vine (m^2)	Lateral LA/ vine (m^2)	Total LA/ vine (m^2)	Yield/ vine (kg)	Clusters /vine (n)	Cluster mass (g)	Berry mass (g)
SHW-WW	10.5b	80b	216	296 b	1.06 b	1.09 a	2.15 b	1.54	15b	104.02a	1.56a
SHW-WS	11b	86b	242	328b	1.13 b	1.23 a	2.36 b	1.63	17b	95.42a	1.52ab
VSP-WW	12ab	242a	253	495 a	2.31 a	0.98 a	3.29 a	1.35	22a	69.39b	1.43ab
VSP-WS	13ab	248a	173	421 a	2.37 a	0.67 b	3.04 a	1.52	20a	67.16b	1.34b
Pergola-WW	15.5a	267a	227	494 a	2.17 a	0.68 b	2.85 a	1.43	18ab	84.2ab	1.48ab
Pergola-WS	16a	302a	173	475 a	2.45 a	0.51 b	2.96 a	1.40	19ab	79.3ab	1.49ab
Sig.	**	**	ns	**	**	*	**	ns	*	*	*

Within column, mean separation was performed by DMRT, P = 0.01.

did not significantly differ for any canopy geometry.

Expressing gas exchange rates per leaf area unit slightly changed the above scenario (Fig. 6A–F), which verified VSP as the most susceptible to a water stress limitation (45% less NCER/LA and 37.6% less T/LA versus the respective well-watered controls). However, for the two remaining canopy types, the P system improved its performance as

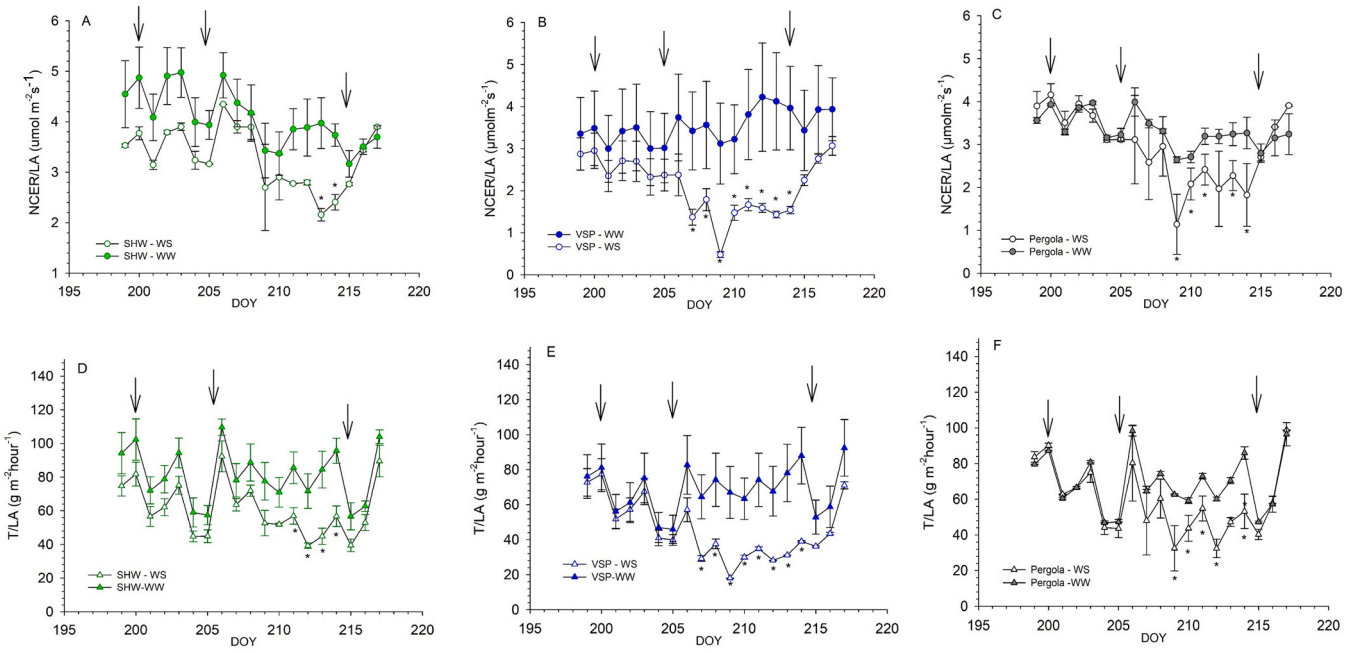

Fig. 6. Seasonal patterns of NCER/LA for SHW (A), VSP (B) and Pergola (C) and of T/LA for SHW (D), VSP (E) and Pergola (F) recorded at the experimental site during the water deficit and rewatering periods (DOY 200–217). Data in each panel were subjected to repeated measure ANOVA analysis and mean separation within date or timing was performed by Fisher test (P = 0.05) only when the time x treatment interaction was significant (P = 0.01). Asterisks indicate which dates resulted in significant differences between water stressed (WS) and well-watered (WW) treatments within each canopy geometry. Vertical bars represent standard errors (SE) around the means (n = 3). Panel A - time x treatment interaction: F = 2.88, P = 0.003; panel B - time x treatment interaction: F = 15.3, P = 0.001; panel C - time x treatment interaction: F = 3.02, P = 0.002; panel D - time x treatment interaction: F = 3.29, P= 0.01; panel E - time x treatment interaction: F = 16.5, P = 0–001 and panel F - time x treatment interaction F = 6.38, P = 0.001. From left to right, arrows indicate beginning of first and second water stress periods and final rewatering.

NCER/LA and T/LA reductions in the WS treatments were 17.0% and 19.7% than WW, whereas SHW showed a 21.9% decrease in NCER/LA and 27.1% decrease in T/LA when compared to WW.

Diurnal NCER/LA trends averaged over first and second period of water stress and over the final rewatering are reported in Fig. 7A-I and, as far as the 50% reduction of water supply and rewatering are concerned, repeated measure analysis showed no significant between-treatment and hour x treatment interactions for any canopy geometry. Conversely, diurnal NCER/LA patterns averaged over the 35% water supply period (Fig. 7D–F) showed differential behavior for each canopy type, clearly distinguishing between SHW vs. VSP and P. The former had overall a mild limitation in NCER/LA (-14% vs the WW vines), whereas in VSP, NCER/LA dropped to 1.61 $\mu molm^{-2}s^{-1}$ from the 3.39 $\mu molm^{-2}s^{-1}$ measured in the non-stressed treatment (-52.5%). In P, this reduction was 41.3% as WS vines scored 1.79$\mu mol\ m^{-2}s^{-1}$, and WW set at 3.39 $\mu mol\ m^{-2}s^{-1}$.

Diurnal T/LA trends (Fig. 8A–I) essentially reflected those described for NCER/LA. The repeated measure ANOVA indicated a lack of a significant hour x treatment interaction for any canopy over the first stress period (Fig. 8A–C) and the rewatering period (Figure G–I). Instead, data taken during the more severe water stress period (DOY 205–214) confirmed significant differences between the WW and WS treatments and higher variability among canopy geometries in terms of dynamic and severity of water stress (Fig. 8D–F). Over the severe stress period comprised between DOY 200–216, T/LA in SHW decreased by 22.7% in the WS vines, whereas such percentage increased to 48.3% and 41.7% in VSP and Pergola, respectively. VSP and P geometries also had a higher number of daytimes during which T/LA in WS was significantly lower than the water loss recorded in WW.

When diurnal variation in WUE was plotted for each canopy geometry x water regime combination (Fig. 9A), no significant between-treatment differences as well as hour x treatments interactions were found over the first stress (Fig. 9A–C) and rewatering (Fig. 9G–I). Conversely, especially during the late morning hours of the severe stress period, canopy WUE was lower in the WS vines of VSP and P thrice and twice a day, respectively (Fig. 9D–E).

3.4. Correlations between gas exchange and environmental and physiological variables

Regardless of the canopy geometry, a negative exponential equation with three parameters was a very close fit (R^2 = 0.97–0.98) for the total direct light data regressed over NCER/LA over the well-watered period (Fig. 10A). When the same correlation was run against T/LA, a linear model proved adequate (R^2 = 0.85–0.88) to fit the data (Fig. 10B), as no further accuracy was reached by running non-linear models.

This scenario substantially changed when air VPD was used as the independent variable (Fig. 10, C, D). A significant linear model was fit between VPD and NCER/LA in each canopy type (Fig. 10C) which, however, was less accurate than that where total direct light was on the x-axis. Moreover, slopes of linear regressions reported in panels B, C and D, did not differ according to the two-tailed t test. Notably, the relationship between VPD and T/LA was closely fit by linear models (R^2 = 0.93–0.96) in any training system (Fig. 10D).

The same correlation types were also checked for data taken during the severe water stress period (Fig. 11A–I). As far as the correlations of total direct light vs. NCER/LA and T/LA are concerned (Fig. 11A–C), the type and accuracy of the fitted models for WW and WS did not differ among canopy geometries and if compared to the pre-stress data set. However, slope analysis performed along the linear portion of the light response curves (interval between 0 and 400 $\mu mol\ m^{-2}s^{-1}$) showed a significant difference for VSP at the two-tailed t-test (p = 0.020). When the test was run over the whole T/LA data sets, slopes were different for both VSP (P = 0.0000) and P (P = 0.0027) but not for SHW. When air VPD was used as an independent variable, the same situation held (i.e., all data sets were fitted by a linear model) although: in the case of VSP (Fig. 11E), the slope of the lines fitted to WW and WS statistically differed for either NCER/LA (p = 0.0353) and T/LA (p = 0.000),

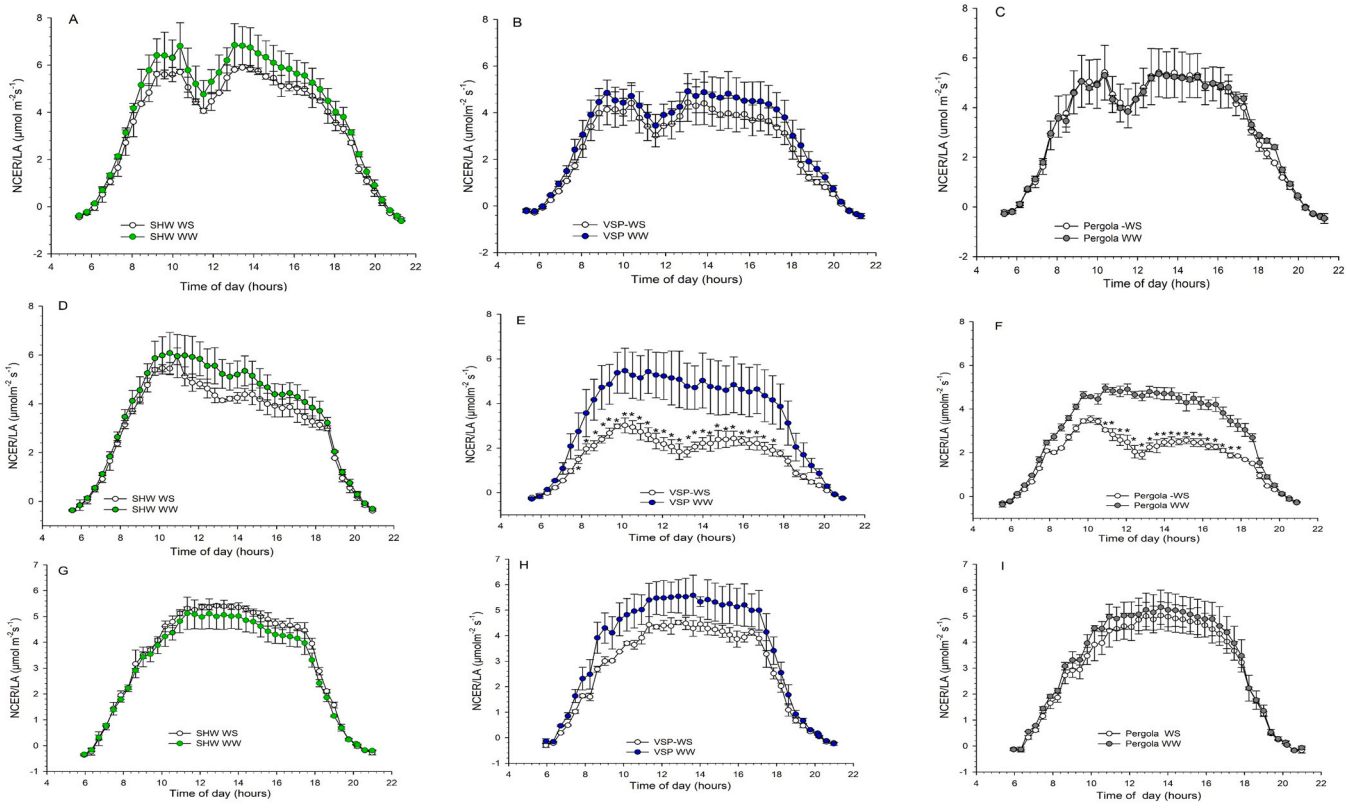

Fig. 7. Durnal (dawn to dusk) pattern of NCER/LA averaged over first stress period (top row, DOY 200–204), second stress period (middle row, DOY 205–214) and rewatering period (bottom row, DOY 215–217). Panels A, D and G refer to SHW – WS and SHW-WW; panels B, E and H refer to VSP- WS and VSP-WW and panels C, F and I refer to Pergola WS and Pergola WW. Data in each panel were subjected to repeated measure ANOVA analysis and mean separation within date or timing was performed by Fisher test (P = 0.05) only when the time x treatment interaction was significant (P = 0.01). Panels D-F: time x treatment interaction: F = 2.755, P = 0.001. Asterisks indicate which dates resulted in significant differences between water stressed (WS) and well-watered (WW) treatments within each canopy geometry. Data reported in panels A-C and G-I were ns. Vertical bars represent standard errors (SE) around the means (n = 3).

whereas for the Pergola (Fig. 11F) slopes of the two fitted lines differed for T/LA only (P = 0.000).

Correlations were also drawn, in each canopy form, for modeled TCLI over the whole-pre stress period (DOY 179–199, Fig. 12A–C) and the whole rewatering period (DOY 215–217, Fig. 12D–F) versus measured NCER/vine and T/vine averaged over the same time windows. In SHW, a sigmoid model was a very good predictor (R^2 = 0.90) of NCER/vine for the earlier data set while the same model equation, albeit significant, was less accurate (R^2 = 0.64) when fitted to the T/vine data (Fig. 12A). VSP displayed no correlation (Fig. 12B), whilst in the Pergola form NCER and T/vine fit a sigmoid model with high accuracy (R^2 = 0.88 for NCER/vine and 0.93 for T/vine). Correlations run over the whole rewatering period (Fig. 12D–F) confirmed in SHW a good sigmoid correlation between modeled TCLI and NCER/vine (R^2 = 0.78) and a looser one (R^2 = 0.50) vs. T/vine. VSP confirmed its lack of significant correlations (Fig. 12E), and in Pergola, a sigmoid model maintained a very good accuracy at predicting NCER/vine (R^2 = 0.90) and T/vine (R^2 = 0.93) (Fig. 12F).

3.5. *Vegetative growth, yield, grape composition, and vine balance*

Vegetative growth components determined at harvest support a differential behavior of SHW vs. VSP and P (Table 1). SHW had a lower final leaf area per vine (2.26 m^2 if pooled over WW and WS treatments), yet lateral leaf area represented 51% of this amount. Final LA in VSP and P was 3.16 m^2 and 2.91 m^2, respectively, with the lateral component accounting for 26% and 20%. Conversely, yield per vine was uniform across canopy forms, and the overall small clusters did not suffer any apparent limitation due to the period of water stress. As per final grape maturity is concerned (Table 3), an overall gradient of more advanced ripening was seen moving from SHW to P, which showed higher TSS, pH, anthocyanins and phenolics, and lower TA. For most ripening parameters VSP showed an intermediate behavior. Such ripening patterns are overall linked to the highest LA/F recorded in P and VSP vs SHW. When canopy efficiency was evaluated as total sugars/vine, however, canopy geometries did not differ.

4. Discussion

The discussion will be initially provided about the differential behavior of the three canopy geometries in terms of NCER, T, and WUE.

While slightly higher seasonal NCER/vine and T/vine rates recorded in VSP and P essentially reflect their higher leaf area (Petrie et al., 2023), it was theoretically unexpected, in terms of diurnal NCER recorded during the WW period, to observe a diurnal pattern that, despite obvious variation in modeled TCLI (Fig. 2) was very constant and similar with NCER peaks to be reached mid-morning and then maintained until mid-afternoon (Fig. 3D, F). This is especially puzzling in the VSP, where no consistent midday drop was seen, which also explains why the correlation between NCER and modeled light interception was quite poor. This outcome has been already seen in the past on NS or close to NS-oriented canopies grown under different conditions and latitudes (Intrieri et al., 2015; Escalona et al., 2016; Poni et al., 2014; Prieto et al., 2020), whereas in two other studies (Petrie et al., 2023, 2009) carried out on NS-oriented Sauvignon blanc rows, the measured temporary NCER depression was milder than the one expected from modeled and intercepted radiation patterns.

This behavior of VSP-trained vines with a close-to-NS orientation has

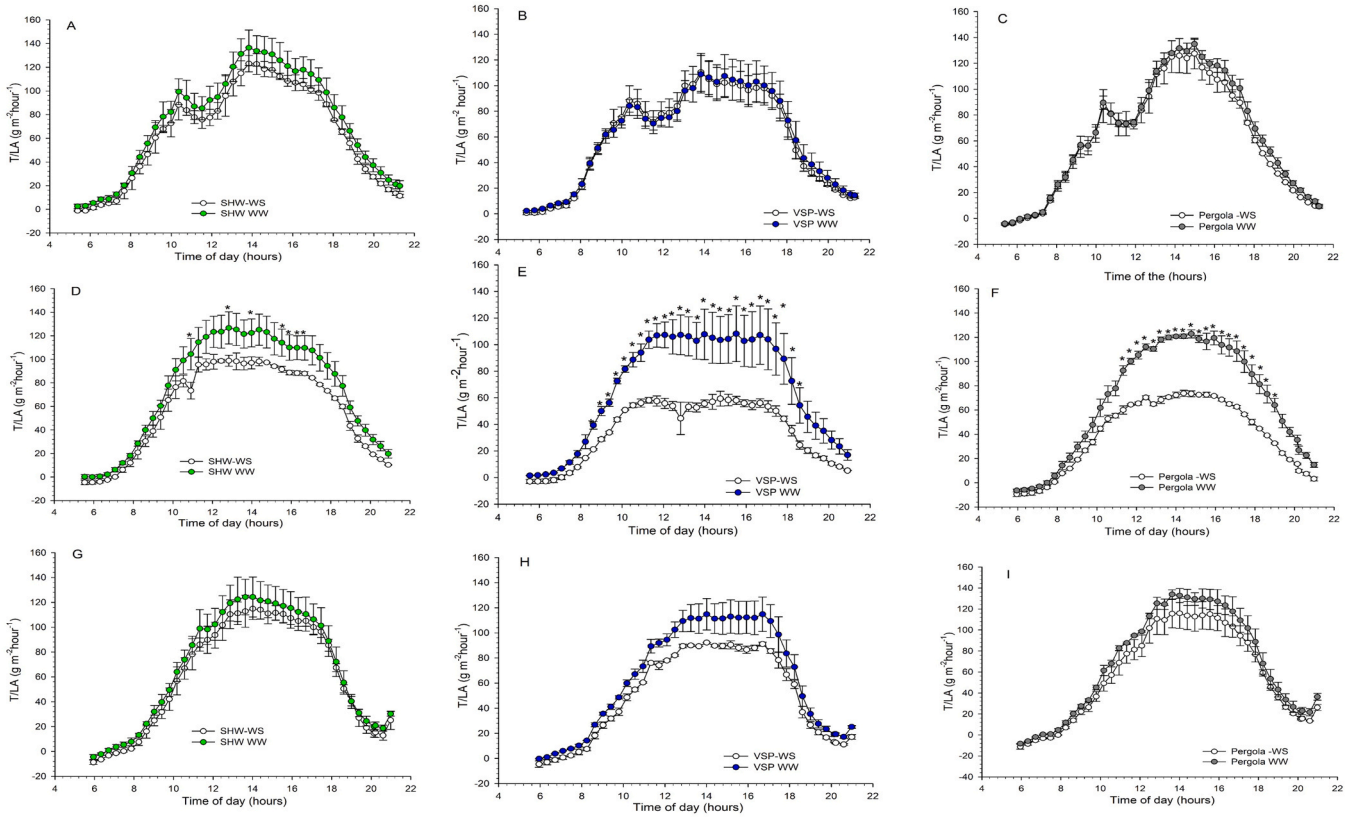

Fig. 8. Diurnal (dawn to dusk) pattern of T/LA averaged over first stress period (top row, DOY 200–204), second stress period (middle row, DOY 205–214) and rewatering (bottom row, DOY 215–217). Panels A, D and G refer to SHW – WS and SHW-WW; panels B, E and H refer to VSP- WS and VSP-WW and panels C, F and I refer to Pergola WS and Pergola WW. Data in each panel were subjected to repeated measure ANOVA analysis and mean separation within date or timing was performed by Fisher test (P = 0.05) only when the time x treatment interaction was significant (P = 0.01). Panels D-F: time x treatment interaction: F = 3.139, P = 0.001. Asterisks indicate which dates resulted in significant differences between water stressed (WS) and well-watered (WW) treatments within each canopy geometry. Data reported in panels A-C and G-I were ns. Vertical bars represent standard errors (SE) around the means (n = 3).

at least two relevant implications: (i) predicting NCER potential based on geometrical VSP features, such as canopy height or width, is unlikely to give realistic estimates and (ii) the capacity of NS-oriented canopies to yield maximum NCER even at high solar angles and minimum light interception, strengthen the hypothesis that available diffuse light at that time is enough to bring the canopy to photosynthetic saturation. Similarly, Petrie et al., (2009) hypothesized and proposed higher quantum yield for light response curves plotted over an overcast day than a clear day. In our study, overcast or mostly cloudy days were a total rarity, yet modeled diffuse light at two dates (Fig. 2) showed that, during the central hours of the day, diffuse light hitting the canopy was slightly higher than 1000 μmol s^{-1} in that exceeding the sum of direct light that reached the horizontal and vertical planes of the canopy. Most interestingly, light response curves (i.e., total direct light vs. NCER/LA) drawn for VSP over the pre-stress period (Fig. 10A) had the same pattern, accuracy, and light saturation point of the other canopy geometries setting at about 800–1000 μmol m^{-2} s^{-1} (Smart, 1974). This means that total direct light is an excellent estimator of NCER regardless of canopy geometry and diurnal changes in the fraction of light interception.

We are unaware of any previous work investigating the gas exchange pattern of sprawl or heavily sloped (pergola) canopies. As per NCER/LA is concerned, canopy types tightly fit to a typical light response curve without apparent deviations from VSP (Fig. 10A). However, SHW and P closely correlated between NCER/vine and modeled light interception (Fig. 12A, C, D, F), which, on one side, is indeed useful if preliminary assessment of the photosynthetic potential of such canopy shapes is needed, and, on the other, displays a major difference between the two training systems. Despite the model fit to the data being the same (a sigmoid curve with three parameters), the increasing patterns of NCER/vine with increasing modeled TCLI are different: in SHW, it is more gradual as a likely result of a canopy type, which, regarding the interaction between row orientation and sun angle, has an overall rounded shape; in P, conversely, there is an abrupt rise in NCER/vine (five- to six-fold compared to early morning values) taking place for modeled TCLI comprised between 1800 and 2200 μmol s^{-1} (8–10 AM) due to the interaction of row direction, sun angle, and the extent of canopy slope. Notably, NCER/vine in P did not show any further increment despite modeled TCLI reaching and exceeding the threshold of 3000 μmol s^{-1} for central and early afternoon hours (Fig. 2). This demonstrates that under specific site conditions, a pergola canopy type is soon oversaturated by the available radiation load.

T/LA again regressed over the total direct light fed the hypothesis of different regulation mechanisms. The best-fit model changed from negative exponential (Fig. 10B) to linear with a modest decrease in accuracy yet, most importantly and irrespective of canopy geometry, when the same direct PAR values (i.e 700 μmolm^{-2} s-1) were reached in the morning and afternoon, the resulting T/LA could also vary by two-fold. Then, other factors are involved in the canopy transpiration response and air VPD then comes into play. When VPD was correlated to NCER/LA in the three training systems, the behavior previously described for T/LA vs. total direct light (Fig. 10C), amplified in magnitude leading to a further decrease in model accuracy. The same VPD values reached in the morning or the afternoon (i.e., 2 kPa) led to a three- to four-fold difference in NCER/LA; such a bias was almost annulled when VPD was regressed over T/LA, as, for any canopy geometry, a very close linear fit (R^2 = 0.93–0.96) was found (Fig. 10D). Moreover, the correlation of modeled TCLI vs. T/vine was excellent for the Pergola.

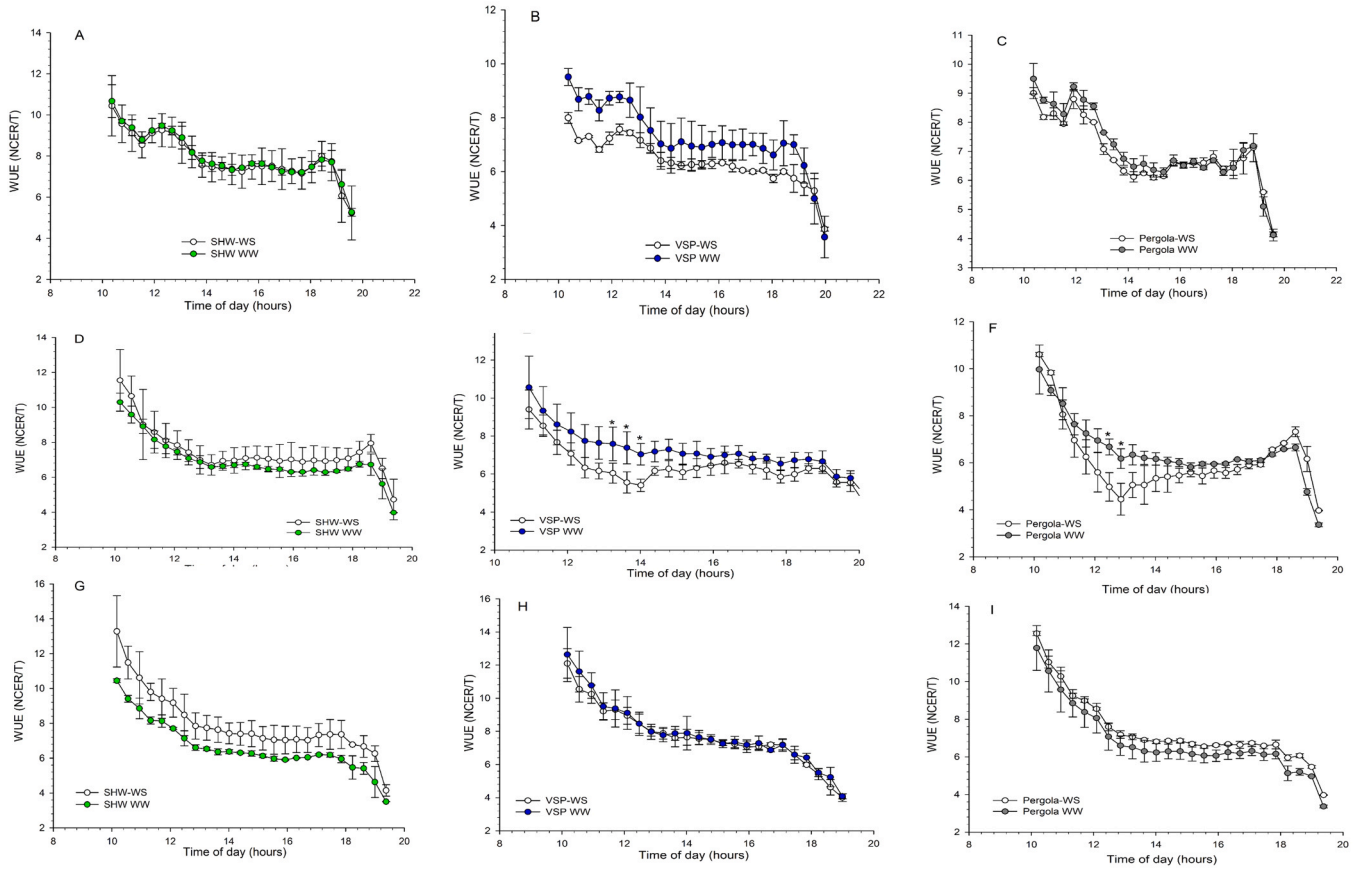

Fig. 9. Diurnal (dawn to dusk) pattern of canopy WUE (NCER/T) averaged over first stress period (top row, DOY 200–204), second stress period (middle row, DOY 205–214) and rewatering (bottom row, DOY 215–217). Panels A, D and G refer to SHW – WS and SHW-WW; panels B, E and H refer to VSP- WS and VSP-WW and panels C, F and I refer to Pergola WS and Pergola WW. Data in each panel were subjected to repeated measure ANOVA analysis and mean separation within date or timing was performed by Fisher test (P = 0.05) only when the time x treatment interaction was significant (P = 0.01). Panels D-F: time x treatment interaction: F = 2.034, P = 0.001. Asterisks indicate which dates resulted in significant differences between water stressed (WS) and well-watered (WW) treatments within each canopy geometry. Vertical bars represent standard errors (SE) around the means (n = 3). Due to high WUE variability early in the morning, time trends start at 10 AM.

The body of these results has at least two main consequences regarding the amount and regulation of water use by different canopy geometries, and, again, the VSP seems to act as a solo player. As also pointed out in a recent paper (Canavera et al., 2023), our data do not dismiss the hypothesis that grapevine water use is a close linear function of the shaded area measured underneath the canopy (Williams and Ayars, 2005). However, calibration provided in the latter study exploited a seasonal variation in the leaf area per vine from 2 to 34 m^2. Moreover, to allow even more variability, the curtains of the trellis were raised for a couple of weeks to resemble an overhead pergola, thereby increasing light interception. However, this did not occur in the current study. We worked on rather static canopies (around 2.5–3.0 m^2 of total leaf area), and the TCLI varied due to the interaction between sun position, canopy geometry, and row orientation. Therefore, in VSP-trained canopies with a close to NS orientation, assuming that canopy water use is the least around solar noon because TCLI is at its minimum would be wrong. Previous work where whole-canopy transpiration was tracked during the day showed that under a precise NS orientation, a mild temporary gap in transpiration can be observed during the central hours of the day, which tracks lower TCLI at that time (Intrieri et al., 1997; Petrie et al., 2023). It is inherent that a model that can include diurnal variability in its TCLI estimation due to row orientation or soil slope is more accurate than any other approach that considers an average daily TCLI estimated from a quite impersonal crop coefficient.

The other main outcome is that VPD was the main driver of T/vine regardless of canopy geometry. On a strict physiological basis, this accords with previous work employing single-leaf (Rogiers et al., 2011; Soar et al., 2006) or whole-canopy approaches. Lu et al. (2003) have shown that VPD either explained most of the variation in canopy conductance and that the rate of leaf transpiration or leaf stomatal conductance was driven by VPD, especially under high soil moisture (Rogiers et al., 2011), or when referred to isohydric cultivars, such as Grenache (Soar et al., 2006). That VPD is such a tight regulator of canopy water loss is likely a matter of concern under a global warming scenario where atmospheric evaporative demand during the summer has been showing a quite steady increase (Garcia-Tejera et al., 2023; Van Leeuwen et al., 2019), as it would lessen chances that evapotranspiration can be controlled by varying, for instance, canopy geometry and orientation.

Our data also allow us to answer an intriguing question: “At the same leaf area level, how is canopy geometry able to affect light use efficiency?” Expressing data on a per leaf area unit basis has undoubtedly revealed that SHW achieves higher photosynthetic efficiency. The increase in NCER/LA found, on a seasonal and diurnal basis, is 24% compared to the other trellises and extraordinarily similar to the same amount (25%) that Intrieri et al. (1997) found when an initially spreading canopy was constrained between foliage wires to reduce thickness and reconduct it to a typical VSP shape. Among the reasons for this difference, as also postulated by Petrie et al. (2009), if the light better penetrates the inner of the canopy, basal leaves receive a higher amount of mostly diffuse radiation which is typically located within the steep linear part of the light response. However, it cannot be ruled out

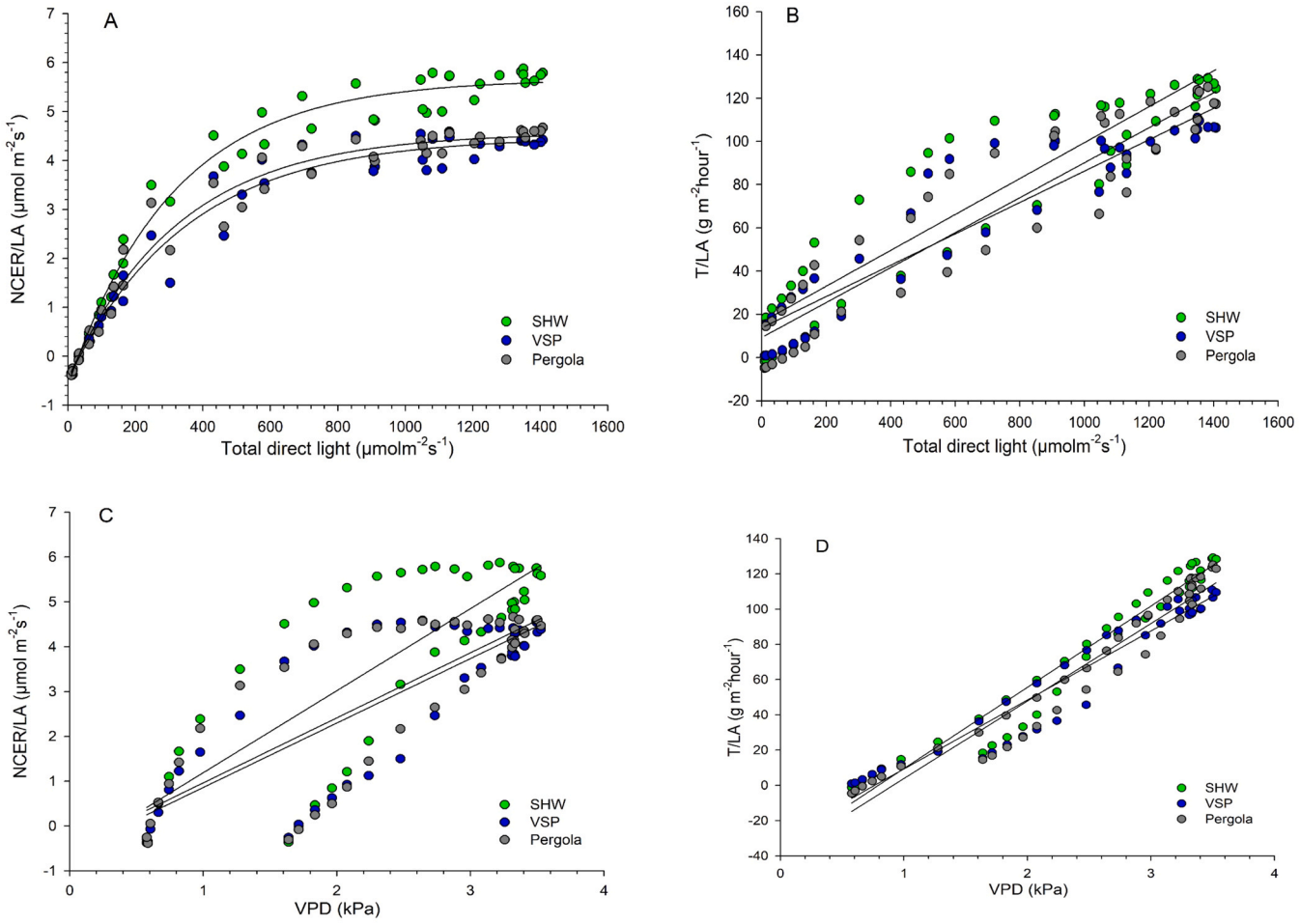

Fig. 10. Correlations between total direct light (PAR as µmol $m^{-2}s^{-1}$) and NCER/LA (A) and T/LA (C) and between air VPD (kPa) and NCER/LA (B) and T/LA (D) for data averaged over the pre-stress period (DOY 179–199) for the three canopy geometries: in A, equations fitted to the data were: y = −0.599+6.263(1-exp(-0.0032x)), R^2 = 0.98 (SHW); y = −0.481+4.956(1-exp(-0.0029x)), R^2 = 0.97 (VSP); y = −0.461+5.029(1-exp(-0.0031x)), R^2 = 0.97 (Pergola). In B: y = 1.8302x – 0.614, R^2 = 0.66 (SHW); y = 1.438x – 0.5794, R^2 = 0.64 (VSP); y = 1.4509x – 0.4861, R^2 = 0.63 (Pergola); in C: y = 0.0831x + 16.33, R^2 = 0.85 (SHW): y = 0.0726x + 13.669, R^2=0.88 (VSP); y = 0.0809x + 9.2206, R^2 = 0.88 (Pergola). In D: y = 46.128x −36.64, R^2 = 0.96 (SHW); y = 43.99x – 40.179, R^2 = 0.94 (VSP): y = 39.166x – 29.99, R^2 = 0.93 (Pergola).

that the measured higher NCER/LA rates can also depend on an overall younger canopy (the proportion of lateral LA to total LA in SHW was 51.4% vs. 25.9% and 20.5% in VSP and P, respectively) and, thus, chances to hold higher NCER rates, especially in the second part of the season (Poni and Giachino, 2000). Finally, the spreading nature of the canopy in SHW facilitates leaf movement under windy conditions, which are likely more impeded in a canopy having foliage wires. Intrieri et al. (1995) showed that light frequency higher than 5 Hz resulted in NCER rates very close to those found under continuous light of high intensity.

Expressing seasonal and diurnal T rates on a per LA area basis also reversed the position of canopy geometry, as SHW registered the highest rates without, however, reaching statistical differences (Fig. 4C,D). However, calculated canopy WUE, which, of course, does not change in its absolute value as a function of unit expression (per vine or LA) indicates that SHW retained the highest rate, which, when evaluated on a diurnal basis within the time window comprised between 10:00 a.m. and 6:00 p.m. (Fig. 3H) occasionally showed significant difference compared to the two other forms. The main reason could be attributed to the higher WUE of basal (internal) leaves reached by a higher amount of diffuse light (PAR between 0 and 400 µmol m^{-2} s^{-1}), which would increase NCER more than proportionally than the T increase.

When the amount of water supplied daily to the vines during the first and second stress periods was compared to actual water use recorded over the whole-pre-stress period, fractional T/vine replenishment corresponded to 79%, 65%, and 69% for SHW, VSP, and P over the first-time frame and to 55%, 45% and 48% SHW, VSP and P over the second. Albeit caution must be used when comparing water stress studies carried out in pots and the field, the overall mild stress shown in all training systems from DOY 200–204 accords with a body of literature, suggesting that supplying 60–70% of actual evapotranspiration does not significantly impair gas exchange (Chaves et al., 2007; Keller et al., 2016; Tarara et al., 2011; Williams and Heymann, 2015). Moreover, similar results were obtained when the water shortage was applied under growing conditions very similar to those used in our study (Merli et al., 2015; Poni et al., 2009). For gas exchange data normalized over the total leaf area and averaged over the second stress period, VSP and P showed a more than two-fold decrease in NCER/LA and T/LA than SHW on a diurnal basis (Fig. 6). However, when the seasonal behavior of the three canopy forms included also the first stress period, SHW and P had similar performances, whereas VSP was again the worst performing. Overall, it can be concluded that over a gradual water stress period, VSP had the worst performance, SHW was the best, and P showed a somewhat intermediate behavior.

The physiology underlying this ranking is not simple and literature does not help: if it is assumed that both VSP and P concentrate their foliage in a canopy volume of limited thickness (30–40 cm), and SHW, conversely, shows a more spreading canopy, the question is why a

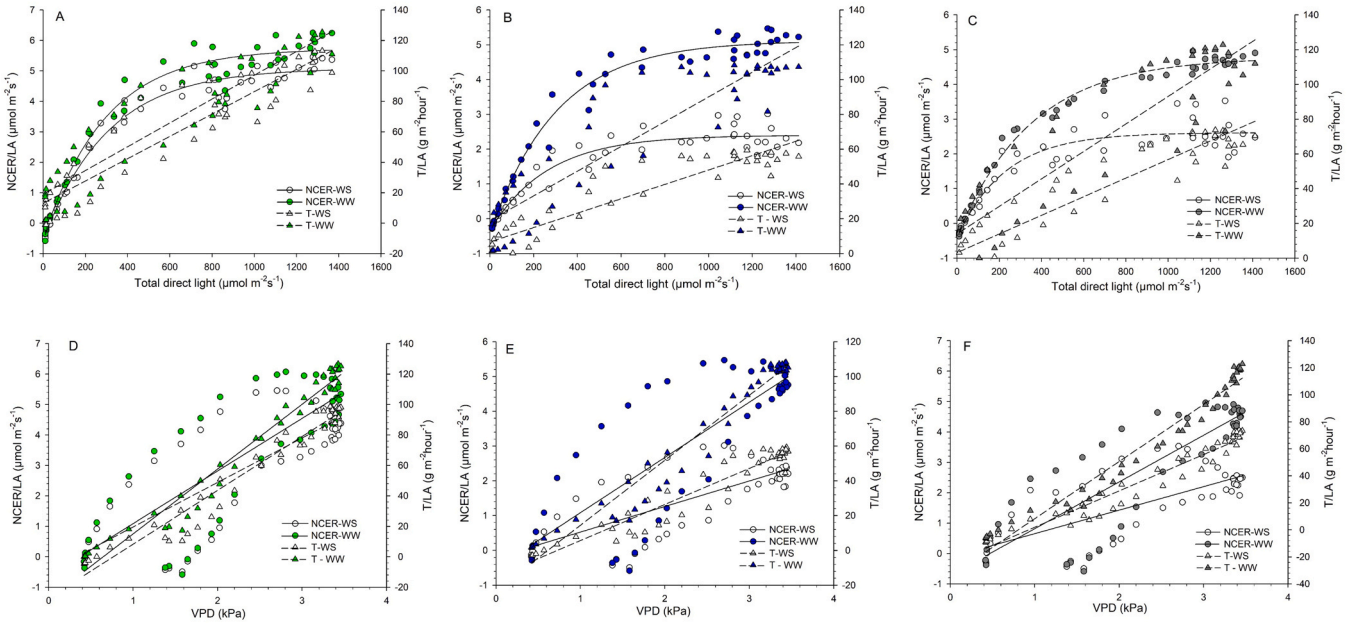

Fig. 11. Upper panels: correlations between total direct light (PAR as µmol $m^{-2}s^{-1}$), NCER/LA and T/LA for well-watered (WW) and water stressed (WS) SHW (A), VSP (B) and Pergola (C) vines for data averaged over the second period of water stress (DOY 205–2014). Lower panels: correlations between air VPD (kPa), NCER/LA and T/LA for well-watered (WW) and water stressed (WS) SHW (D), VSP (E) and Pergola (F) for data averaged over the second period of water stress (DOY 205–214). In A, equations fitted to the data were: $y = -0.4656+6.0026(1-exp(-0.0030x))$, $R^2 = 0.97$ (NCER/LA-WW); $y = -0.5264+5.2211(1-exp(-0.0034x))$, $R^2 = 0.95$ (NCER/LA-WS); $y = 0.0809x + 20.1557$, $R^2 = 0.83$ (T/LA – WW); $y = 0.0682x + 11.83$, $R^2 = 0.85$ (T/LA – WS). In B: $y = -0.4371+5.5542(1-exp(-0.0033x))$, $R^2 = 0.98$ (NCER/LA-WW); $y = -0.3360+2.7373(1-exp(-0.0038x))$, $R^2 = 0.91$ (NCER/LA-WS); $y = 0.0711x + 18.95$, $R^2 = 0.82$ (T/LA – WW); $y = 0.0414x + 6.6618$, $R^2 = 0.85$ (T/LA – WS). In C: $y = -0.3811+5.158(1-exp(-0.0029x))$, $R^2 = 0.99$ (NCER/LA-WW); $y = -0.4056+3.018(1-exp(-0.0038x))$, $R^2 = 0.88$ (NCER/LA-WS); $y = 0.0791x + 13.97$, $R^2 = 0.79$ (T/LA – WW); $y = 0.0536x + 3.206$, $R^2 = 0.87$ (T/LA – WS). In D: $y = 1.7276x -0.6370$, $R^2 = 0.64$ (NCER/LA-WW); $y = 1.4596x -0.4780$, $R^2 = 0.59$ (NCER/LA-WS); $y = 42.584x -27.43$, $R^2 = 0.96$ (T/LA – WW); $y = 35.36x -27.04$, $R^2 = 0.96$ (T/LA – WS); In E: $y = 1.5889x -0.5064$, $R^2 = 0.63$ (NCER/LA-WW); $y = 0.7334x -0.2053$, $R^2 = 0.51$ (NCER/LA-WS); $y = 37.3729x -22.9278$, $R^2 = 0.96$ (T/LA – WW); $y = 20.7204x -15.0416$, $R^2 = 0.92$ (T/LA – WS). In F: $y = 1.5379x -0.7213$, $R^2 = 0.69$ (NCER/LA-WW); $y = 0.7731x -0.1191$, $R^2 = 0.47$ (NCER/LA-WS); $y = 42.289x -34.0175$, $R^2 = 0.96$ (T/LA – WW); $y = 26.8881x -24.9378$, $R^2 = 0.95$ (T/LA – WS). In panel B slope comparison by two tailed t test was significant for NCER-WW vs NCER-WS quantum yield assessment ($P = 0.020$) and for T/WW vs T/WS ($P= 0.006$). In C, two-tailed t test was significant only for T/WW vs T/WS slope comparison ($P= 0.0027$). In panel D, slope comparisons were ns; in E, WW had different slopes as compared to WS for either NCER/LA ($P = 0.053$) and T/LA ($P = 0.000$), whereas in F slopes were different only for T/WW and T/WS ($P = 0.000$).

progressive water shortage has a greater impact in the restricted canopy types than in the sprawl type. The magnitude of such impact is quantified by the variation in diurnal canopy WUE, which, under stress, was not changed in SHW, whereas it showed generally lower values in VSP-WS and P-WS vs. their respective well-watered controls reaching significance at few dates in the late morning-early afternoon (Fig. 9E,F). During the time frame between noon and 2:00 p.m., we have the highest radiation and a still rising VPD and the lower canopy WUE in VSP-WS, and P-WS is caused by a temporary drop of NCER/LA, which then resumes after 1:30 p.m. The hypothesis is that after the early morning irrigation, high radiation load and high VPD have caused in these canopy geometries a more severe transient water stress, which was then relieved by the second daily irrigation.

Fig. 11 feeds, however, an additional hypothesis about the differential behavior of the tested canopy geometries under water stress. When looking at the light response curves of WW and WS treatments, it is clear that while the light saturation point was not affected in SHW, the same was almost halved at about 500–600 µmol $m^{-2}s^{-1}$ in VSP and P vs. the 1000–1200 µmol$m^{-2}s^{-1}$ of their respective well-watered vines (Fig. 11A-C). However, mechanisms involved seem to differ. In VSP, the quantum yield calculated over the linear part of the light response curves was significantly reduced in WS and this certainly contributed to the lower maximum NCER/LA reached at saturation (WS had a 32.8% reduction vs WW). In Pergola, the comparison between initial slope of the light response curves did not reach statistical significance, yet maximum NCER/LA at saturation was curtailed by about 45% as compared to WW suggesting that, under stress, in this trellis continuous exposure to high light and temperature was quite impactful. Changes in light response curves similar to those described above take place when comparing the photosynthetic performance of sun and shade leaves (Bertamini et al., 2004; Greer and Weedon, 2012; Palliotti and Poni, 2015) or when a severe drought occurs eventually associated to light and thermal stress (Carvalho et al., 2016; Escalona et al., 2000; Maroco et al., 2002). In the last connection, it has been shown that P_n limitation is always caused by the coexistence of stomatal and non-stomatal effects, the latter including reductions in electron transport, CO_2 carboxylation efficiency, and utilization of triose-P capacity, significantly reducing the maximum photosynthetic rates and quantum yield at light and CO_2 saturation conditions (Maroco et al., 2002). In our study, the extent of stomatal limitation can be inferred by comparing slopes of the linear total direct light vs T/LA relationship in WW and WS, which, for VSP and P, significantly differed, implying that this gap widened along with increasing light availability (Fig. 11). A similar response was seen when the same relationships were plotted against air VPD.

Our data did not indicate that whole-canopy WUE is significantly enhanced under drought conditions either on a seasonal (Fig. 5J-L) and a diurnal (Fig. 9A-F) basis (Keller et al., 2016). This strengthens previous data (Medrano et al., 2015; Merli et al., 2015; Poni et al., 2009), showing that the correlation between instantaneous WUE usually derived from single-leaf readings of assimilation and transpiration vs. canopy WUE is usually low, being worse with increasing water stress. The main reason for such a mismatch has been explained as interference due to a change in the position of a single leaf at the time of measurement (i.e., seeking, for instance, exposure to saturation light) than whole canopy readings,

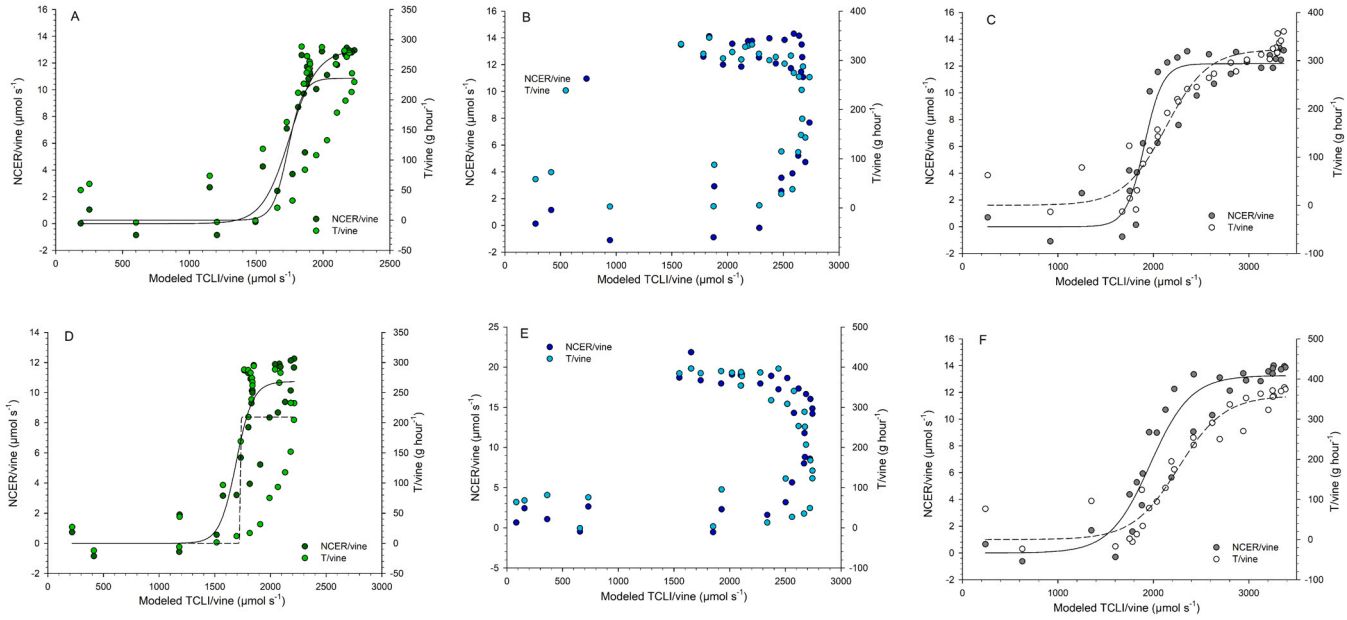

Fig. 12. Correlations between modeled TCLI/vine (μmol s^{-1}) and NCER/vine and T/vine calculated for the whole pre-stress period (DOY 179–199) and rewatering period (DOY 215–217). From left to right, panels A-C refer to SHW, VSP and Pergola, respectively (first date). Panels D-F refer to SHW, VSP and Pergola, respectively (second date). Data were fit to the following equations: panel A – y = 12.96/(1+exp(-(x –1750.89)/101.95)), R^2 = 0.90 (NCER/vine); y = 235.90/(1+exp(-(x – 1737.81)/56.31)), R^2 = 0.64 (T/vine). In C: y = 12.17/(1+exp(-(x – 1906.22)/96.73)), R^2 =0.88 (NCER/vine); y = 323.31/(1+exp(-(x – 2130.98)/220.36)), R^2 =0.93 (T/vine). In D: y = 10.73/(1+exp(-(x – 1691.45)/74.82)), R^2 = 0.78 (NCER/vine); y = 209.45/(1+exp(-(x – 1730.28)/213.00)), R^2 = 0.50 (T/vine) In F: y = 13.26/(1+exp(-(x – 1967.72)/211.83)), R^2 = 0.90 (NCER/vine); y = 358.65/(1+exp(-(x – 2264.29)/239.35)), R^2 = 0.93 (T/vine). Data shown in panels B and E were ns.

Table 3
Grape composition and vine balance determined at harvest on potted cv. Sangiovese vines trained of Single High Wire (SHW), Vertical Shoot Positioned (VSP) and Pergola canopies under Well-Watered (WW) and Water Stress (WS) irrigation regimes.

Treatments (T)	TSS (°Brix)	TSS (g/vine)	TA (g L^{-1})	pH	Total Anthocyanins (mg g^{-1})	Total Phenols (mg g^{-1})	LA/Y ratio (m^2/kg)
SHW-WW	19.56c	301.2	8.05 a	3.19 b	0.298c	1.81c	1.40b
SHW-WS	20.13 bc	328.1	8.30 a	3.23 b	0.359 bc	1.98 bc	1.45b
VSP-WW	19.14c	258.4	8.18 a	3.16 b	0.499 ab	2.00 bc	2.11a
VSP-WS	20.47 abc	311.1	7.94 a	3.11 b	0.492 ab	1.92 bc	1.95a
Pergola-WW	21.89 ab	313.0	5.33b	3.41 a	0.525 ab	2.16 b	2.30a
Pergola-WS	22.60 a	316.4	5.49b	3.42 a	0.608 a	2.51 a	2.17a
Sig.	**	ns	***	***	***	***	**

Within column, mean separation was performed by DMRT, P = 0.01.

allowing to catch the integral of many leaves measured under their natural position.

While we are conscious that vine performance assessment based on a single year of data and referred to semi-controlled conditions might represent an indeed partial data set, the vine yield components, and grape composition determined at harvest seem robust enough to forward a preliminary evaluation. Under the encouraging scenario of very uniform yield per vine across treatments, two results seem to stand out: at the same harvest date, P vines retained more ripened fruits (higher TSS, pH, color and phenolics, lower TA) than VSP, especially, SHW; when overall canopy efficiency is evaluated as total accumulated sugars in the clusters, no significant differences were shown. While the lower grape quality performance reached in SHW, once assessed that the LA/Y was not limiting for full ripening (Kliewer and Dokoozlian, 2005; Poni et al., 2018) is a likely consequence of more competitive laterals shoots triggered by the early trimming, it is more complicated to explain why P shows higher pH and lower TA than VSP when, in theory, P should cast more shade onto clusters and, thus, slow down at least malic acid degradation. However, any horizontal or heavily sloped canopy wall typically shows a higher seasonal and daily radiation load than any VSP trellis (Palliotti and Poni, 2015). Both the darkening of individual leaves and the exposure to high light intensities can induce or accelerate senescence in various crops, and it has been proposed that changes in the redox status of cells associated with the overproduction of reactive oxygen species (ROS) might be the basis of the senescence symptoms (Pintó-Marijuan and Munné-Bosch, 2014; Sakuraba, 2021). In the grapevine, it has been shown that Sangiovese leaves grown and maintained under continuous high light until the age of 113 days have shown a marked accelerated senescence vs. leaves of the same age, which, however after full expansion had experienced shade periods, varying from 17 to 45 days in length (Palliotti and Poni, 2015). It is also well known that earlier leaf senescence would promote the re-translocation of nutrients into nearby organs, including clusters (Cahoon, 1985; Rogiers et al., 2017). As already shown in the grapevine (Mpelasoka et al., 2003), potassium, the most abundant ion, can be responsible for the rise in pH and decrease in TA observed, in the current case, in the Pergola vines.

With overall whole-canopy efficiency assessed as total sugars/vine, the three canopy forms showed a quite similar potential, which is not surprising. Vine balance can also be expressed by replacing LA used as a numerator in the leaf area-to-yield ratio with the likely more reliable mean daily carbon uptake over the entire experiment (DOY 179–249).

This resulted to be 8.11, 8.68, and 8.10 μmol vine^{-1} s^{-1} for SHW, VSP, and P, respectively, therefore explaining the quite similar efficiency of a per vine basis. Then, a hypothesis of upgrading to a soil unit surface (hectare) basis is needed. Assuming that a free interrow corridor of at least 2.1 m is required for unhindered machine transit regardless of the training system, the ideal between row spacing would be 2.5 m in VSP, 2.7 m in SHW, and 4.6 m in P (the latter assuming a bilateral version). While a 1 m spacing in the row seems appropriate in all cases, the resulting vine density is, respectively, 4000, 3704, and 2174. However, when it comes to the total canopy investment per vine, the P value will double at 4348, to confirm the pergola as the most rewarding choice in the specific environment.

5. Conclusions

A seasonal and diurnal survey of whole-canopy gas exchange behavior under well-watered or water stress conditions was produced for the first time for three relevant canopy geometries in grapevine-growing vertically shoot-positioned, spreading, and pergola-type canopies.

Under well-watered conditions, SHW reached significantly higher NCER/LA rates than the other canopy forms, and diurnal patterns of gas exchange were, especially in VSP, totally unrelated to modeled light interception. Total direct light had a tight correlation with NCER/LA, according to a typical light response curve model regardless of canopy geometries, whereas diurnal VPD was the main driver of T/LA according to a tight linear fit. When a progressive water shortage was induced by restricting water supply to 50% and 35% of the initial volume of 4.5 L/vine, while all canopy geometries had an overall mild response compared to the 50% reduction, VSP and P showed higher sensitivity to the imposed water stress than SHW. This latter also manifested in a somewhat reduced canopy WUE in the VSP-WS and P-WS treatments during the late morning hours compared to the respective WW treatments. Under severe water stress, VSP and P also exhibited modifications as lower light saturation points and lower quantum yield. While yield per vine at harvest did not differ, ripening was enhanced in Pergola vs. VSP, and especially in SHW, the latter likely suffering from stronger competition by lateral shoots prompted by the early main shoot trimming.

Preference for one of the three tested geometries might vary depending on the scale of appreciation. If evaluated on a per canopy (vine) basis, the spreading habitus of an SHW trellis is more efficient in terms of higher NCER per LA area unit and higher resilience to a progressive water deficit; if the comparison is taken to a soil surface basis (hectare), the Pergola trellis can assure the most efficient land investment.

Author statements

We the undersigned declare that this manuscript is original, has not been published before, and is not currently being considered for publication elsewhere.

Declaration of Competing Interest

The authors declare that they have no known competing financial interests or personal relationships that could have appeared to influence the work reported in this paper.

Appendix A. Supporting information

Supplementary data associated with this article can be found in the online version at doi:10.1016/j.envexpbot.2024.105716.

References

Bernizzoni, F., Civardi, S., Van Zeller, M., Gatti, M., Poni, S., 2011. Shoot thinning effects on seasonal whole-canopy photosynthesis and vine performance in Vitis vinifera L. cv. Barbera. Aust. J. Grape Wine Res. 17 (3), 351–357.

Bertamini, M., Muthuchelian, K., Nedunchezhian, N., 2004. Photoinhibition of photosynthesis in sun and shade grown leaves of grapevine (Vitis vinifera L.). Photosynthetica 42, 7–14.

Cahoon, G.A., 1985. Potassium nutrition of grapes. Potassium Agric. 1105–1134.

Canavera, G., et al., 2023. A sensorless, Big Data based approach for phenology and meteorological drought forecasting in vineyards. Sci. Rep. 13 (1), 16818.

Carbonneau, A., 1983. Méthodes de mesure simple de la surface foliaire exposée par hectare, élément déterminant du système de conduite de la vigne. OENO One 17 (4), 281–285.

Carvalho, L., Coito, J., Gonçalves, E., Chaves, M., Amâncio, S., 2016. Differential physiological response of the grapevine varieties Touriga Nacional and Trincadeira to combined heat, drought and light stresses. Plant Biol. 18, 101–111.

Chaves, M.M., et al., 2007. Deficit irrigation in grapevine improves water-use efficiency while controlling vigour and production quality. Ann. Appl. Biol. 150 (2), 237–252.

Cola, G., et al., 2014. Description and testing of a weather-based model for predicting phenology, canopy development and source–sink balance in Vitis vinifera L. cv. Barbera. Agric. For. Meteorol. 184, 117–136.

Corelli-Grappadelli, L., Magnanini, E., 1993. A whole-tree system for gas-exchange studies. HortScience 28 (1), 41–45.

Escalona, J.M., et al., 2016. Using whole-plant chambers to estimate carbon and water fluxes in field-grown grapevines. Theor. Exp. Plant Physiol. 28, 241–254.

Escalona, J.M., Flexas, J., Medrano, H., 2000. Stomatal and non-stomatal limitations of photosynthesis under water stress in field-grown grapevines. Funct. Plant Biol. 27 (1), 87-87.

Garcia-Tejera, O., et al., 2023. Viticulture adaptation to global warming: modelling gas exchange, water status and leaf temperature to probe for practices manipulating water supply, canopy reflectance and radiation load. Agric. For. Meteorol. 331, 109351.

Greer, D., Weedon, M., 2012. Photosynthetic light responses in relation to leaf temperature in sun and shade leaves of grapevines. VII Int. Symp. Light Hortic. Syst. 956, 149–156.

Intrieri, C., Zerbi, G., Marchiol, L., Poni, S., Caiado, T., 1995. Physiological response of grapevine leaves to lightflecks. Sci. Hortic. 61 (1-2), 47–59.

Intrieri, C., Poni, S., Rebucci, B., Magnanini, E., 1997. Effects of canopy manipulations on whole-vine photosynthesis: results from pot and field experiments. VITIS-GEILWEILERHOF 36, 167–174.

Intrieri, C., Poni, S., Rebucci, B., Magnanini, E., 2015. Row orientation effects on whole-canopy gas exchange of potted and field-grown grapevines. VITIS-J. Grapevine Res. 37 (4), 147.

Keller, M., et al., 2016. Deficit irrigation alters grapevine growth, physiology, and fruit microclimate. Am. J. Enol. Vitic. 67 (4), 426–435.

Kliewer, W.M., Dokoozlian, N.K., 2005. Leaf area/crop weight ratios of grapevines: influence on fruit composition and wine quality. Am. J. Enol. Vitic. 56 (2), 170–181.

Lakso, A.N., Intrigliolo, D., Eissenstat, D.M., 2007. Modeling concord grapes with" VitiSim", a simplified carbon balance model: understanding pruning effects. VIII Int. Symp. Model. Fruit. Res. Orchard Manag. 803, 243–250.

Lloyd, J., et al., 1995. Measuring and modelling whole-tree gas exchange. Funct. Plant Biol. 22 (6), 987–1000.

Long, S., Hallgren, J., 1985. Measurement of CO2 assimilation by plants in the field and the laboratory. Techniques in bioproductivity and photosynthesis. Elsevier, pp. 62–94.

López-Lozano, R., Baret, F., de Cortázar Atauri, I.G., Lebon, E., Tisseyre, B., 2011. 2D approximation of realistic 3D vineyard row canopy representation for light interception (fIPAR) and light intensity distribution on leaves (LIDIL). Eur. J. Agron. 35 (3), 171–183.

Louarn, G., Dauzat, J., Lecoeur, J., Lebon, E., 2008a. Influence of trellis system and shoot positioning on light interception and distribution in two grapevine cultivars with different architectures: an original approach based on 3D canopy modelling. Aust. J. Grape Wine Res. 14 (3), 143–152.

Louarn, G., Lecoeur, J., Lebon, E., 2008b. A three-dimensional statistical reconstruction model of grapevine (Vitis vinifera) simulating canopy structure variability within and between cultivar/training system pairs. Ann. Bot. 101 (8), 1167–1184.

Lu, P., Yunusa, I.A., Walker, R.R., Müller, W.J., 2003. Regulation of canopy conductance and transpiration and their modelling in irrigated grapevines. Funct. Plant Biol. 30 (6), 689–698.

Mabrouk, H., Sinoquet, H., 1998. Indices of light microclimate and canopy structure of grapevines determined by 3D digitising and image analysis, and their relationship to grape quality. Aust. J. Grape Wine Res. 4 (1), 2–13.

Maroco, J.P., Rodrigues, M.L., Lopes, C., Chaves, M.M., 2002. Limitations to leaf photosynthesis in field-grown grapevine under drought—metabolic and modelling approaches. Funct. Plant Biol. 29 (4), 451–459.

Medrano, H., et al., 2015. From leaf to whole-plant water use efficiency (WUE) in complex canopies: limitations of leaf WUE as a selection target. Crop J. 3 (3), 220–228.

Merli, M.C., et al., 2015. Comparison of whole-canopy water use efficiency and vine performance of cv. Sangiovese (Vitis vinifera L.) vines subjected to a post-veraison water deficit. Sci. Hortic. 185, 113–120.

Mpelasoka, B.S., Schachtman, D.P., Treeby, M.T., Thomas, M.R., 2003. A review of potassium nutrition in grapevines with special emphasis on berry accumulation. Aust. J. Grape Wine Res. 9 (3), 154–168.

Palliotti, A., Poni, S., 2015. Grapevine under light and heat stresses. Grapevine A Chang. Environ.: A Mol. Ecophysiol. Perspect. 148–178.
Peña, J.P., Tarara, J., 2004. A portable whole canopy gas exchange system for several mature field-grown grapevines. VITIS-GEILWEILERHOF 43 (1), 7–14.
Petrie, P.R., Trought, M.C., Howell, G.S., Buchan, G.D., 2003. The effect of leaf removal and canopy height on whole-vine gas exchange and fruit development of Vitis vinifera L. Sauvignon Blanc. Funct. Plant Biol. 30 (6), 711–717.
Petrie, P.R., Trought, M.C., Howell, G.S., Buchan, G.D., Palmer, J.W., 2009. Whole-canopy gas exchange and light interception of vertically trained Vitis vinifera L. under direct and diffuse light. Am. J. Enol. Vitic. 60 (2), 173–182.
Petrie, P.R., Trought, M.C., Howell, G.S., 2023. Influence of scott henry and four-cane vertical shoot positioning training systems and crop load on whole-vine gas exchange of vitis vinifera L. Sauvignon blanc. Am. J. Enol. Vitic. 74 (2).
Pintó-Marijuan, M., Munné-Bosch, S., 2014. Photo-oxidative stress markers as a measure of abiotic stress-induced leaf senescence: advantages and limitations. J. Exp. Bot. 65 (14), 3845–3857.
Poni, S., et al., 2009. Performance and water-use efficiency (single-leaf vs. whole-canopy) of well-watered and half-stressed split-root Lambrusco grapevines grown in Po Valley (Italy). Agric. Ecosyst. Environ. 129 (1-3), 97–106.
Poni, S., et al., 2013. Late leaf removal aimed at delaying ripening in cv. S angiovese: physiological assessment and vine performance. Aust. J. Grape Wine Res. 19 (3), 378–387.
Poni, S., et al., 2014. An improved multichamber gas exchange system for determining whole-canopy water-use efficiency in grapevine. Am. J. Enol. Vitic. 65 (2), 268–276.
Poni, S., et al., 2018. Grapevine quality: a multiple choice issue. Sci. Hortic. 234, 445–462.
Poni, S., Giachino, E., 2000. Growth, photosynthesis and cropping of potted grapevines (Vitis vinifera L. cv. Cabernet Sauvignon) in relation to shoot trimming. Aust. J. Grape Wine Res. 6 (3), 216–226.
Poni, S., Magnanini, E., Rebucci, B., 1997. An automated chamber system for measurements of whole-vine gas exchange. HortScience 32 (1), 64–67.
Poni, S., Intrieri, C., Magnanini, E., 2000. Seasonal growth and gas exchange of conventionally and minimally pruned Chardonnay canopies. VITIS-GEILWEILERHOF 39 (1), 13–18.
Poni, S., Palliotti, A., Bernizzoni, F., 2006. Calibration and evaluation of a STELLA software-based daily CO2 balance model in Vitis vinifera L. J. Am. Soc. Hortic. Sci. 131 (2), 273–283.
Poni, S., Bernizzoni, F., Civardi, S., 2008. The effect of early leaf removal on whole-canopy gas exchange and vine performance of Vitis vinifera L.Sangiovese'. VITIS-GEILWEILERHOF- 47 (1), 1.
Poni, S., Lakso, A., Intrieri, C., Rebucci, B., Filipetti, I., 2015. Laser scanning estimation of relative light interception by canopy components in different grapevine training systems. VITIS-J. Grapevine Res. 35 (4), 177.
Poni, S., Frioni, T., Gatti, M., 2023. Summer pruning in Mediterranean vineyards: is climate change affecting its perception, modalities, and effects? Front. Plant Sci. 14.
Prieto, J.A., et al., 2020. A functional–structural plant model that simulates whole-canopy gas exchange of grapevine plants (Vitis vinifera L.) under different training systems. Ann. Bot. 126 (4), 647–660.
Reynolds, A.G., Heuvel, J.E.V., 2009. Influence of grapevine training systems on vine growth and fruit composition: a review. Am. J. Enol. Vitic. 60 (3), 251–268.
Rogiers, S.Y., Greer, D.H., Hutton, R.J., Clarke, S.J., 2011. Transpiration efficiency of the grapevine cv. Semillon is tied to VPD in warm climates. Ann. Appl. Biol. 158 (1), 106–114.
Rogiers, S.Y., Coetzee, Z.A., Walker, R.R., Deloire, A., Tyerman, S.D., 2017. Potassium in the grape (Vitis vinifera L.) berry: transport and function. Front. Plant Sci. 8, 1629.
Sakuraba, Y., 2021. Light-mediated regulation of leaf senescence. Int. J. Mol. Sci. 22 (7), 3291.
Saxton, K. and Rawls, W., 2016. Soil water characteristics.
Smart, R., 1974. Photosynthesis by grapevine canopies. J. Appl. Ecol. 997–1006.
Smart, R.E., 1985. Principles of grapevine canopy microclimate manipulation with implications for yield and quality. a review. Am. J. Enol. Vitic. 36 (3), 230–239.
Soar, C.J., et al., 2006. Grape vine varieties Shiraz and Grenache differ in their stomatal response to VPD: apparent links with ABA physiology and gene expression in leaf tissue. Aust. J. Grape Wine Res. 12 (1), 2–12.
Tarara, J.M., Peña, J.E.P., Keller, M., Schreiner, R.P., Smithyman, R.P., 2011. Net carbon exchange in grapevine canopies responds rapidly to timing and extent of regulated deficit irrigation. Funct. Plant Biol. 38 (5), 386–400.
Van Leeuwen, C., et al., 2019. An update on the impact of climate change in viticulture and potential adaptations. Agronomy 9 (9), 514.
Williams, L., Ayars, J., 2005. Grapevine water use and the crop coefficient are linear functions of the shaded area measured beneath the canopy. Agric. For. Meteorol. 132 (3-4), 201–211.
Williams, L. and Heymann, H., 2015. Effects of applied water amounts and trellis/training system on grapevine water relations, berry characteristics, productivity and wine composition of 'Cabernet Sauvignon', VIII International Symposium on Irrigation of Horticultural Crops 1150, pp. 413-426.
Winkler, A.J., 1974. General viticulture. Univ of California Press.